PERGAMON

Applied Geochemistry 14 (1999) 197–221

Applied Geochemistry

Lead isotope evidence for recent uranium mobility in geological formations of Brazil: implications for radioactive waste disposal

S. S. Iyer[a,*], M. Babinski[b], M. M. Marinho[c], J. S. F. Barbosa[d], I. M. Sato[e], V. L. Salvador[e]

[a]*Department of Physics and Astronomy, University of Calgary, Calgary, AB Canada T2N 1N4*
[b]*Instituto de Geociências, Universidade de São Paulo, São Paulo, Brazil*
[c]*Companhia Baiana de Pesquisa Mineral (CBPM), Salvador, Brazil*
[d]*Instituto de Geociências, Universidade Federal da Bahia, Salvador, Brazil*
[e]*Instituto de Pesquisas Energéticas e Nucleares (CNEN/SP), São Paulo, Brazil*

Received 9 May 1997; accepted 2 February 1998

Editorial handling by J. C. Petit

Abstract

Lead–lead isotope data from whole rock samples are used to investigate the recent (last few million years) mobility of U and Th. The method is based on the comparison of the calculated present day U and Th concentrations required to yield the Pb isotope composition in the samples with the actual present day concentrations of U and Th obtained by direct measurement. The geological formations studied include the Neoproterozoic carbonate sediments of the Bambuí Group, Archean/Paleoproterozoic granite–greenstone terrain of the Contendas–Mirante Complex and a Proterozoic ortho-gneisses hosting U deposit in Lagoa Real. All these formations are in the São Francisco Craton, Brazil. The data show high U mobility in the carbonate sediments and in the deformed ortho-gneisses set in a ductile shear zone. Infiltration of groundwater through fault zones seems to have facilitated the U mobility. The Pb isotope approach is a useful technique complementing U-series disequilibrium studies and may be included for site characterization studies for radioactive waste disposal.

1. Introduction

Long term disposal of high level radioactive waste is a great challenge facing the scientific community today (Ahearne, 1997; Han et al., 1997). Disposal in chosen geological formation is the preferred option. However, the long term stability or residence time of the radioactive elements in geological formations is a matter of concern. Under oxidizing conditions U becomes hexavalent uranyl ions (UO_2^+), which forms water soluble compounds. The studies of the mobility of the fission products and the transuranic actinides in geological formations is possible only through the study of natural chemical equivalents (Chapman and Smellie, 1986). Such analogous elements are: trivalent light REE for Am, Cm and Pu (III); U(IV) and Th(IV) for Pu(IV) and Np(IV) (Chapman and Smellie, 1986; Menager et al., 1992). Thus a thorough understanding of the conditions controlling the mobility of uranium in geological formations is important for the disposal of radioactive waste (Gascoyne et al., 1995; Kastenburg and Granton, 1997).

In this present study mobility of U and Th in contrasting geological formations is investigated using the Pb isotope data. Since the radioactive isotopes ^{238}U,

* Corresponding author. E-mail: iyer@acs.ucalgary.ca.

0883-2927/99/$ - see front matter
PII: S0883-2927(98)00040-7

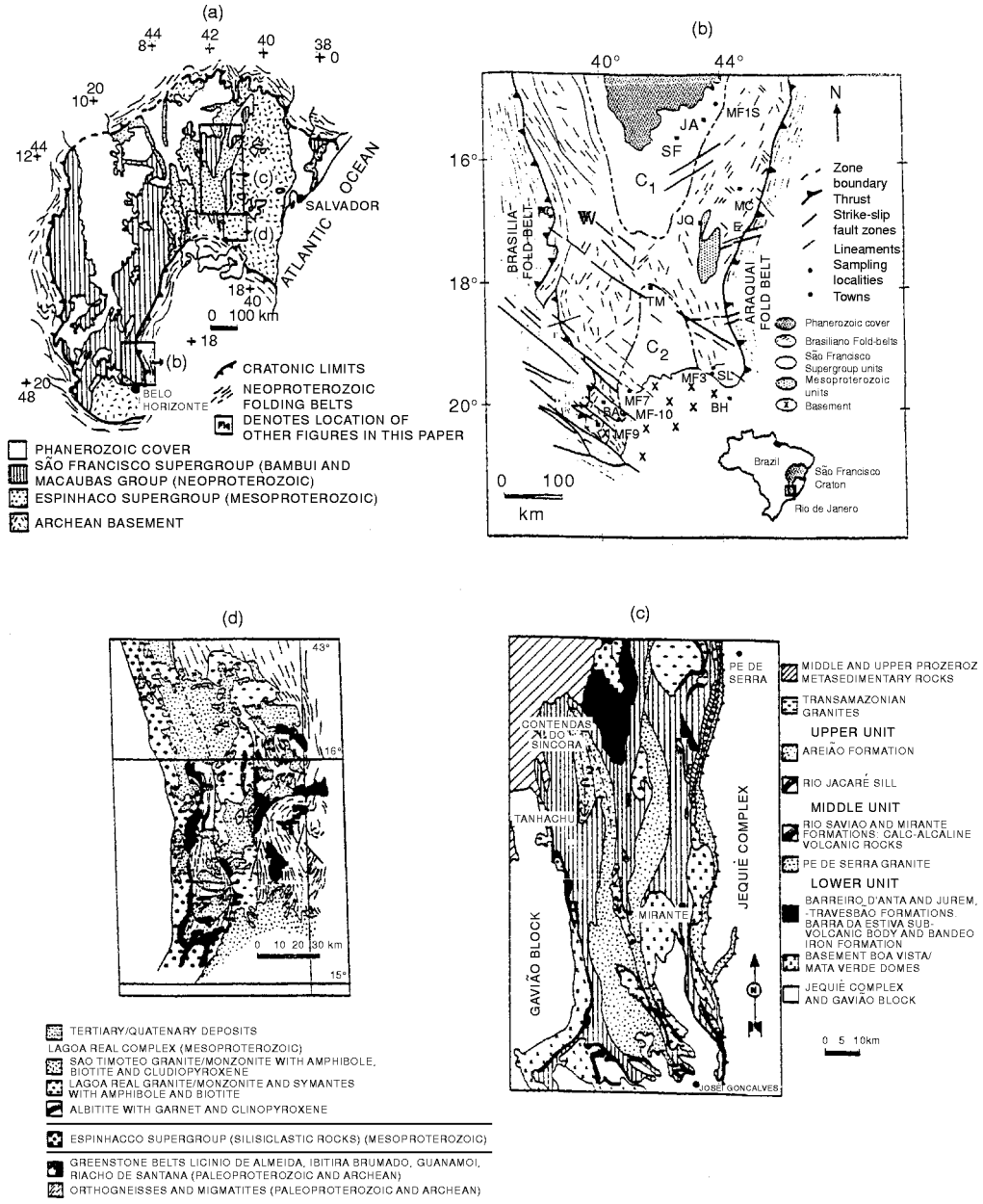

Fig. 1. Geographical locations and geological maps of the areas investigated. (a) Locations of the Bambuí Group, ContendasMirante Complex and Lagoa Real Complex. (b) Geological and structural map of the southern portion of the São Francisco Basin (modified from Chemale et al., 1993). W = zone affected by Brasília Fold belt, E = zone affected by Araçuaí Fold belt, C_1 and C_2= undeformed zones. BA = Bambuí. PI = Piumhi, JQ = Jequitaí JA = Januaria, PC = Paracatu,, MC = Montes Claros, SF = São Francisco, BH = Belo Horizonte, TM = Três Marias. (c) Geological map of the Contendas Mirante Complex, Bahia, Brazil (modified from Marinho, 1991). (d) Geological map of the Lagoa Real Complex (modified from Barbosa and Dominguez, 1996).

^{235}U and ^{232}Th decay to stable isotopes of Pb, the abundance of the radiogenic isotopes ^{206}Pb, ^{207}Pb and ^{208}Pb provides a direct measure of their parent isotopes under closed system conditions. In many cases the isotope evolution of Pb through geological time can be precisely modeled and the $\mu(^{238}U/^{204}Pb)$, as well as $\kappa(^{232}Th/^{204}Pb)$ values can be established at different stages of the geological history. The determination of the non-radiogenic Pb isotope ^{204}Pb then provides the necessary reference datum in order to establish the U

and Th concentrations in the rock. A comparison of these calculated values with the measured U and Th contents for the same samples can then show the recent loss or gain of these elements. The radioactive disequilibriun studies (Ivanovich and Harmon, 1987) are employed to investigate the mobility of radioactive elements and they yield information on the mobility over the past 10^6 a. The Pb isotope approach may provide information over larger time span of the order of 50×10^6 a (Rosholt et al., 1973) and an estimate of the time span covered by the Pb isotope approach is discussed in Appendix A. The Pb isotope approach may serve as a complementary tool to radioactive disequilibrium investigations.

The study focuses on the Archean granite–greenstone terrain of the Contendas–Mirante Complex (Bahia), Neoproterozoic carbonate rocks of the Sete Lagoas formation, Bambuí Group and the Lagoa Real granite–orthogneiss Complex, all in the São Francisco Craton, Brazil (Fig. 1(a)). The geological formations studied include both crystalline rocks and sedimentary formations. The rock formations of the Contendas–Mirante Complex were investigated as possible Brazilian nuclear waste disposal sites. The Lagoa Real Complex may be considered a natural analogous granite formation, because of the nature of the U mineralization associated with hydrothermal fluid circulation (Kerrich, 1986a,b). In the Bambuí Group carbonates are associated with organic matter formed during primary biosynthesis (Iyer et al., 1992, 1995). The presence of organic matter in the Oklo natural fission reactor appears to have helped in the immobilization of U and fission products (Nagy et al., 1993). The recent mobility of U and Th in these 3 formations of the São Francisco Craton is determined from the Pb isotope data. The data reported in this study are generated as a part of a regional geochronological investigation and are being applied in studies of U (and Th) mobility.

2. Geological setting

2.1. Bambui Group, São Francisco Basin

The rocks of the São Francisco Basin are deposited on the Archean and Paleoproterozoic basement of the São Francisco Craton (Almeida, 1977), and this basin represents an extensive Neoproterozoic sedimentary cover (more than 3×10^5 km^2), composed of clastic and carbonate sequences. This is an intracratonic basin deformed by the marginal Brasiliano (650 to 500 Ma) fold belts (Fig. 1(b)).

The sedimentary rocks of the basin comprise the São Francisco Supergroup and are divided into Macaúbas Group (and correlative units) and the overlying Bambuí Group. The Macaúbas Group consists of diamictites, shales and quartzites, and contains record of a wide spread glacial event. In the northern portion an age of 1.0 Ga has been attributed to this glacial event (D'Agrella Filho et al., 1990; Renne et al., 1990).

The contact between the Bambuí Group and the Macaúbas Group is generally tectonic. The Bambuí Group is divided into 5 formations (Dardenne, 1978), from the base to the top: Sete Lagoas, Serra de Santa Helena, Lagoa de Jacaré, Serra da Saudade and Três Marias. The lower most unit (Sete Lagoas Formation) contains the thick stromatolitic carbonate sequence deposited in shallow marine water conditions. Lead isotope data from the Sete Lagoas Formation is discussed in this study. The São Francisco Basin is bordered by Brasiliano Fold Belt. The tectonics that gave rise to this fold belt deformed the sedimentary rocks of the basin, especially on the basin's borders, where lower greenschist metamorphic conditions are reached. The metamorphic grade as well as the deformation decrease towards the center of the basin, where the rocks are anchimetamorphic in grade and preserve the original sedimentary structures. Based on structural studies, Alkmim et al. (1989) and Chemale et al. (1993) divided the southern part of the São Francisco basin into 3 domains, according to the intensity of deformation (Fig. 1(b)): the Western part (W), affected by the Brasilia Fold Belt; the eastern part (E), affected by Araçuaí Fold Belt and the central part (C_1 and C_2), where the rocks are undeformed. Most of the northern part of the basin is covered by Phanerozoic sediments.

Lead–lead ages determined on the carbonate rocks from the Sete Lagoas Formation are in the interval of 690 to 520 Ma (Babinski, 1993). Older ages in the interval of 870 to 820 Ma were also obtained, but the errors were large (~250 Ma). Most of the Rb–Sr and K–Ar ages fall in the 500 to 700 Ma interval (Bonhomme, 1976; Thomaz Filho and Bonhomme, 1979; Parenti Couto et al., 1981; Bonhomme et al., 1982) and these ages are considered to represent the resetting of the isotope system during Brasiliano Deformation. The Brasiliano Deformation has wide spread impact in the São Francisco Craton resetting the isotopic clocks (Cordani et al., 1992).

2.2. Contendas–Mirante Complex

The Contendas–Mirante Complex is made up of supracrustal formations, metamorphosed to greenschist facies in the western part and progressively changing eastward to amphibolite facies (Fig. 1(c)). Rock samples from two units of the Contendas–Mirante sequence have been investigated for their radioactive element concentrations. The geological settings of the units and their petrography are discussed below.

2.2.1. Calc–alkaline volcanic rocks

These calc–alkaline volcanic rocks form an intercalation in the schist and also crop out as a continuous layer that borders the western side of the mafic–ultramafic body known as the Rio Jacaré Sill. The volcanic rocks are of two types: metabasalts and andesites. The metabasalts are massive or amygdaloidal, fine grained, foliated and are represented by an essentially quartzoze polygonal mosaic with a lesser amount of plagioclase. These basalts are composed of amphiboles (composition between Mg and Fe hornblende), sometimes with cummingtonite halos, plagioclase (An 33–40%) and rare opaque minerals (ilmenite and magnetite). The andesites are greenish–gray, foliated, fine grained and composed of amphibole (composition between Mg and Fe hornblende). The andesites generally contain oriented clinopyroxene and smaller proportions of sphene and zircon within a granoblastic mosaic of plagioclase (An 31–37%) and quartz.

2.2.2. Pé de Serra granite

This granite body is 100 km long with a maximum width of 5 km. It crops out along the north–eastern border of the Contendas–Mirante belt and appears to be intrusive in the volcanic–sedimentary sequence. It comprises two rock types, the first sub-alkaline and the second alkaline (Marinho, 1991). The first type has oriented granoblastic texture, represented by a fine grained mosaic composed of saussuritized plagioclase (An 17–20%), clear microcline and quartz with anhedral to sub-hedral bluish–gray to pale reddish brown amphibole associated with abundant sphene crystals. In some places this granite has a very fine grained mosaic with relict crystals of plagioclase and microcline. These finer grained varieties are richer in green biotite and epidote. The second type of granite comprises alkaline granites and syenites with aegirine and andradite. The alkaline rock has heterogranular hypidiomorphic and sometimes oriented aegirine, commonly associated with andradite and sphene, within a medium grained mosaic essentially composed of albite (An 1–2%) in hypidiomorphic grains with exsolution of K-feldspar. Large quantities of microcline and subordinate amounts of quartz are also present in the mosaic.

The geochronological studies yielded T_{DM} Nd model age of 3.1 Ga and Rb–Sr ages between 2.5 to 2.2 Ga for the sub-alkaline rocks, while a Pb–Pb isochron age of 2.3 Ga and a T_{DM} Nd model age of 3.1 Ga were obtained for the alkaline rocks (Marinho, 1991).

2.3. Lagoa Real Granite–Orthogneiss Complex

Lagoa Real is one of the largest U sites in Brazil with several ore bodies comprising a combined ore reserve of the order of 10^5 metric tons of U_3O_8 (Villaça, 1982). The Lagoa Real Granite–Orthogneiss Complex (Fig. 1(d)) lies in the N central part of the São Francisco Craton (Almeida, 1977; Cordani and Brito Neves, 1982). The main rock types in the Lagoa Real Complex are the São Timoteo granite, orthogneisses (probably formed from the deformation of the São Timoteo granite), other ortho-gneisses representing intercalation of the old basement, albitites and amphibolites. The mineralogical composition of these rock types are described in Cordani et al. (1992). The lenticular albitite bodies occur within the deformed part of the complex along a slightly arcuate structure with a length of about 100 km and submeridional orientation. Some of these albitites, containing pyroxene + garnet, are the main host of U mineralization.

The exact relationship between albitization and U mineralization remains unclear (Stein et al., 1980; Lobato et al., 1982; Turpin et al., 1988). Although the microcline gneisses do not host economic U mineralization, a few have anomalous (50–200 ppm) U contents. Stein et al. (1980) called attention to the possibility that the present disposition of the mineralization may be the result of reconcentration of U along faults reactivated during the Brasiliano (Pan-African) Cycle. A hypothesis formulated by Lobato et al., (1982) and Lobato and Fyfe (1990) involves the release of a mineralizing fluid in response to overloading of the basement and granitic rocks on to the Mesoproterozoic Espihnaço sedimentary sequence via a thrust mechanism during the Brasiliano Cycle. Fluid inclusion (Fuzikawa et al., 1988), geochemical (Maruejol et al., 1987) and geochronological data (Turpin et al., 1988, Cordani et al., 1992) do not support the model of overthrusting.

Geochronological investigations using Rb–Sr whole rock, U–Pb zircon, Pb–Pb whole rock, Sm–Nd whole rock, K–Ar minerals have been carried out by Turpin et al. (1988) and Cordani et al. (1992). Using the data Cordani et al. (1992) summarized the geochronological evolution of the Lagoa Real Complex (Table 1). According to Cordani et al. (1992) the initial albitization and U mineralization may have occurred at around 1.52 Ga ago, during the Espinhaço tectono–metamorphic event, which was accompanied by strong hydrothermal–metasomatic activity. Finally widespread remobilization of U occurred during the Brazilian Orogeny, between 820 to 500 Ma.

3. Experimental Techniques

Lead isotope measurements have been carried out by mass spectrometric methods, whereas U and Th measurements have been carried out by mass spectrometric isotope dilution method and WD-X-ray

Table 1
Summary of radiometric dates and geological events of the Lagoa Real Complex (Turpin et al., 1988; Cordani et al., 1992)

Age (Ma)	Isotopic clock	Geological event
2760	Rb–Sr whole rock isochron	Formation of the basement rocks
1700	U-Pb zircon (Concordia)	Formation of granitoid rocks
	Pb-Pb whole rock isochron	(São Timoteo granite)
	Rb-Sr whole rock isochron	
1500–1200	U-Pb zircon (Concordia)	Regional metamorphism,
		Formaton of ortho-gneisses, albitites and related
	Rb–Sr disturbed system	rocks
	Sm–Nd	U mineralization,
800–550	U–Pb uranium minerals	Regional thermal event
	K–Ar minerals	Final U mineralization and metasomatism

Fluorescence technique. The analytical details are given in Marinho (1991), Cordani et al. (1992) and Babinski (1993).

4. Lead–lead Isotope Dating And Radioactive Element Distribution

The Pb–Pb dating of the rocks and minerals is based on the decay of ^{238}U, ^{235}U and ^{232}Th and the equations employed are:

$$(^{206}Pb/^{204}Pb)_0 = (^{206}Pb/^{204}Pb)_i + (^{238}U/^{204}Pb)_0[e^{\lambda t} - 1] \quad (1)$$

$$(^{207}Pb/^{204}Pb)_0 = (^{207}Pb/^{204}Pb)_i + (^{235}U/^{204}Pb)_0[e^{\lambda' t} - 1] \quad (2)$$

$$(^{208}Pb/^{204}Pb)_0 = (^{208}Pb/^{204}Pb)_i + (^{232}Th/^{204}Pb)_0[e^{\lambda'' t} - 1] \quad (3)$$

where subscripts 0 and i represent the values at time $t = 0$ (today) and $t = i$ (initial).

λ, λ' and λ'' are the radioactive decay constants of ^{238}U, ^{235}U and ^{232}Th respectively.

In the Pb–Pb isochron method a plot of $^{207}Pb/^{204}Pb$ Vs $^{206}Pb/^{204}Pb$ for cogenetic rocks with the same initial ratios yields a straight line, from the slope of which the age "t" is calculated. Along with "t", the model μ_1 ($^{238}U/^{204}Pb$) value is also calculated from the intercept of the isochron and the geochron (the line connecting the primordial Pb isotope ratios and the present day Pb isotope ratios) lines (Stacey and Kramers, 1975). The μ_1 is generally used to determine the source region of Pb, for example, mantle, lower crust and upper crust (Faure, 1986).

In order to calculate the present day radioactive-element concentrations in individual rock samples it is necessary to model their Pb isotope evolution and calculate the $(^{206}Pb/^{204}Pb)_i$ and $(^{208}Pb/^{204}Pb)_i$ values. The $(^{206}Pb/^{204}Pb)_i$ value is calculated from the equation

$$(^{206}Pb/^{204}Pb)i = (^{206}Pb/^{204}Pb)pr + \mu_1[e^{\lambda T} - e^{\lambda t}] \quad (4)$$

where $(^{206}Pb/^{204}Pb)pr$ is the primordial ratio ($=9.307$) and T is the age of the earth (4.57 Ga). The present day $(^{238}U/^{204}Pb)_0$ value is obtained by substituting the $(^{206}Pb/^{204}Pb)i$ value (from Eq. (4)) and the computed isochron age "t" in Eq. (1). This modeling may be extended to thorogenic Pb to determine the $(^{232}Th/^{204}Pb)_0$ values. The elemental concentration of Pb is measured for each sample and expressed in terms of the molar concentration of ^{204}Pb. Using the ^{204}Pb molar concentration the present day abundances of ^{238}U, ^{235}U and ^{232}Th can be calculated. A comparison of these values with the U and Th concentrations measured in the rocks (obtained by mass spectrometric isotope dilution or X-ray fluorescence methods) shows the extent of gain or loss of U and Th suffered by the sample. The calculation procedure is illustrated in the Appendix B with an example.

5. Results and discussion

5.1. Neoproterozoic Carbonates of Sete–Lagoas Formation, Bambuí Group

Lead isotope data for samples taken from 5 outcrops in the Sete Lagoas Formation of the Bambuí Group (Fig. 1(b)) are used to determine the Pb–Pb isochron age values and the present day U and Th concentrations in these samples. The significance of the age data and the U, Th concentrations of each outcrop is briefly outlined.

5.1.1. MF 7 outcrop

Carbonate samples belonging to horizontal layers of the Sete Lagoas Formation were collected from 4 profiles within an abandoned quarry. Although samples were fractured, they did not show any evidence of

Table 2
Lead isotope data of carbonate samples from the MF 7 outcrop, Bambui Group, Brazil (Babinski, 1993)

Sample number	$^{206}Pb/^{204}Pb$	$207Pb/^{204}Pb$	$^{208}Pb/^{204}Pb$	Pb(ppm)	U(ppm)	Th(ppm)	U(ppm)*	U Loss (%)
MF-7-G1-L1	26.974	16.159	38.5				0.69	
MF-7-G1-L2	28.821	16.298	38.465	0.62	0.90	0.44	0.65	27
MF-7-G1-L3	29.481	16.33	38.456					
MF-7-G1-L4	29.941	16.365	38.543					
MF-7-G1-L5	31.26	16.406	38.463	0.88	1.49	0.60	0.95	36
MF-7-G2-L1	27.121	16.222	38.617	0.46	0.58	0.36	0.59	-1
MF-7-G2-L2	28.773	16.487	38.982	0.17	0.24	0.15	0.42	-73
MF-7G2-L3	30.235	16.393	38.529	0.53	0.84	0.38	0.55	35
MF-7G2-L4	30.612	16.401	38.51	0.5	0.81	0.35	0.54	34
MF-7G2-L5	31.629	16.463	38.528	0.75	1.29	0.53	0.67	48
MF-7G3-WR	27.173	16.158	38.382	0.45	0.57	0.31	0.43	25
MF-7G4-L1	27.174	15.974	37.745	0.43	0.55	0.19	0.65	-17
MF-7G4-L2	32.964	16.53	38.553	0.51	0.94	0.36	0.7	26
MF-7G6-L2	33.784	16.584	38.592	0.54	1.04	0.38	0.74	29
MF-7H1-L1	27.217	16.156	38.27	0.25	0.32	0.16	0.68	-112
MF-7H1-L2	29.458	16.363	38.371	0.35	0.53	0.23	0.6	-13
MF-7H1-L3	31.821	16.503	38.39	0.49	0.85	0.32	0.71	17
MF-7H1-L4	32.058	16.588	38.59	0.59	1.04	0.43	0.53	49
MF-7H1-L5	36.109	16.702	38.339	0.62	1.33	0.37	0.95	28
MF-7H2-L1	26.79	16.228	38.44	0.22	0.27	0.16	0.65	-140
MF-7H2-L2	30.323	16.467	38.511	0.17	0.27	0.12	0.38	-40
MF-7H2-L3	32.753	16.557	38.441	0.23	0.42	0.15	0.53	-26
MF-7H2-L4	32.101	16.529	38.53	0.38	0.67	0.27	0.64	5
MF-7H2-L5	37.216	16.889	38.627	0.25	0.56	0.17	0.54	3
MF-7H3-WR	28.093	16.284	38.392	0.32	0.44	0.22	0.38	13
MF-7H4-L1	24.19	16.01	38.396	0.37	0.35	0.27	0.51	-47
MF-7H4-L2	29.812	16.378	38.353	0.38	0.59	0.25	0.55	7
MF-7H5-WR	28.514	16.29	38.344	0.3	0.42	0.20	0.41	3
MF-7H6-WR	28.267	16.293	38.386	0.29	0.40	0.20	0.4	1
MF-7H7-L2	29.954	16.42	38.525	0.23	0.36	0.16	0.3	16
MK-7K1-L2	26.911	16.203	38.517	0.31	0.39	0.23	0.28	27
MF-7L1-L2	34.455	16.685	39.209	0.31	0.61	0.28	0.33	46
MF-7L2-L2	33.382	16.591	39.018	0.31	0.58	0.27	0.44	24
MF-7M1c-L2	53.559	17.884	38.663	0.34	1.15	0.20	0.83	28
MF-7M1f-L2	37.754	16.893	38.904	0.23	0.52	0.18	0.22	58
MF-7N1-L2	34.293	16.709	38.674	0.26	0.51	0.19	0.5	2
MF7N2-L2	33.493	16.649	38.648	0.24	0.45	0.18	0.44	3
MF-7O1-L2	41.871	17.081	38.777	0.22	0.57	0.16	0.07	88
MF-7O2-L2	41.441	17.028	38.725	0.26	0.67	0.18	0.22	67
MF-7P1-L2	41.524	17.103	38.766	0.24	0.62	0.17	0.06	90
MF-7P2-L2	38.258	16.91	38.8	0.27	0.62	0.20	0.28	55
MF-7Q1-L2	38.03	16.272	38.308	0.74	1.71	0.43	0.26	85
MF-7Q2-L2	29.918	16.84	39.543	0.66	1.01	0.71	0.33	67
MF-7Q3-L2	28.738	16.295	38.279	0.63	0.91	0.40	0.42	54
MF-7R1-L2	51.531	17.754	39.731	0.23	0.74	0.21	0.06	92
MF-7R2-L2	50.437	17.693	39.739	0.25	0.79	0.23	0.4	49
MF-7S1-L2	22.971	16.016	38.556	0.45	0.36	0.36	0.17	52
MF-7S2-L2	22.762	15.983	38.452	0.54	0.42	0.41	0.23	45
MF-7T1-L2	45.374	17.454	39.145	0.16	0.45	0.13	0.19	58
MF7U1-L2	44.263	17.182	39.64	0.12	0.33	0.11	0.21	36
MF-7U2-L2	38.684	17.696	39.242	0.6	1.39	0.53	0.26	81

Average U (ppm) = 0.64 ± 0.37
Average Th (ppm) = $0.26 \pm .15$
* U measured by IDMS.

mesoscopic deformation. X-ray diffraction studies reveal that the samples are comprised predominantly of calcites with trace amounts of dolomite and quartz. A petrographic study did not reveal any evidence of metamorphism but did show that much recrystallization has occurred and, additionally, that the contacts between mineral grains are generally diffuse because of carbonate dissolution. Lead isotope data from 51 whole rock samples and acid leaches are given in Table 2. For the calculation of the Pb–Pb isochron age only samples L2 were considered as the other samples showed slightly higher analytical blanks. The isochron age obtained was 686 ± 68 Ma (Fig. 2(a)). Although the samples did not show any mesoscopic deformation in thin sections, the evidence of recrystallization (carbonate dissolution etc.) indicates that the rocks are affected by secondary processes. Hence the age of 686 Ma may be considered the minimum age of deposition. The age value is in agreement with the Rb–Sr isochron data obtained for shales from the Bambuí Group (Bonhomme, 1976; Thomaz Filho and Bonhomme, 1979; Thomaz Filho and Lima, 1981).

From the Pb isotope data (Fig. 2(a), (b)) present day U and Th values are calculated (Table 2), the former ranging from 0.4 to 1.8 ppm U (Fig. 2(c)) and the latter from 0.2 to 0.8 ppm (Fig. 2(d)). The Th/U values are generally less than 1. The average U, Th and Th/U values are 0.64 ± 0.37 ppm, 0.26 ± 0.15 ppm and 0.5 ± 0.2 respectively. These values are within the range observed for carbonate rocks in general (Bayer et al., 1978; Pertlik et al., 1978). Concentrations of U in carbonate rocks are similar to those of calcareous organisms, where U substitutes for Ca in the lattice. Generally U concentrations in carbonate rocks are uniform and little variation is seen between calcites and dolomites. Concentrations of Th in carbonate rocks are low, as Th does not enter the carbonate lattice readily. A close relationship between Th content and insoluble residue content of the limestone (Adams and Weaver, 1958) demonstrates that most of the Th in limestones is in the clay or heavy mineral fraction. Consequently the Th/U ratio is generally low.

Concentrations of U calculated using Pb isotope data are compared with the U analyses by isotope di-

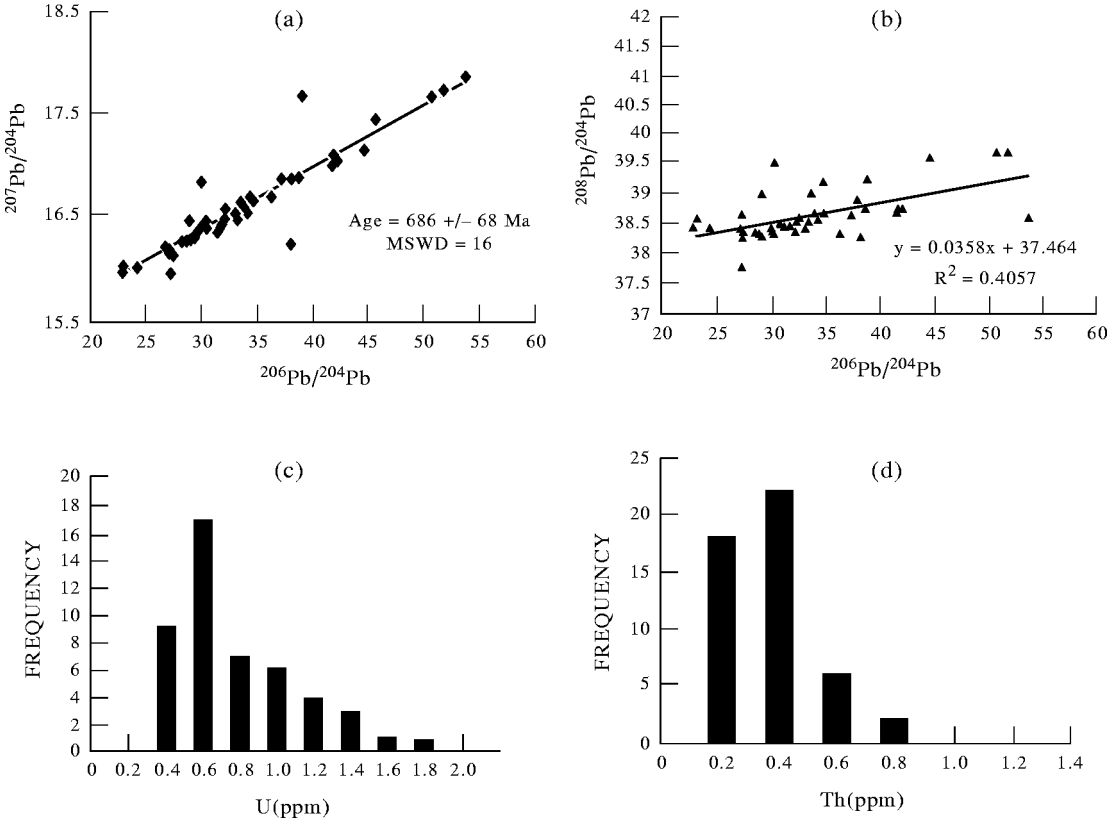

Fig. 2. Pb isotope systematics and U Th distribution in samples from the MF 7 outcrop (Babinski, 1993). (a) $^{207}Pb/^{204}Pb$ vs $^{206}Pb/^{204}Pb$ diagram showing age, μ_1 and MSWD values. (b) $^{208}Pb/^{204}Pb$ vs $^{206}Pb/^{204}Pb$ diagram. (c) Histogram of calculated U contents (ppm). (d).Histogram of calculated Th contents (ppm).

lution mass spectrometry (Fig. 3(a)) which shows that majority of the samples (about 80%) have U losses ranging from 0 to 90% (see also Table 2). The good isochron fit in the $^{207}Pb/^{204}Pb$–$^{206}Pb/^{204}Pb$ diagram, yielding geologically meaningful ages concordant with other isotopic clocks, indicates that the loss of U is recent. Within each profile samples were collected at depth intervals of 50 cm. A plot of the U loss against depth (Fig. 3(b)) shows a reasonably good correlation, with lower loss at greater depth. This correlation may be due to groundwater activity or oxidizing conditions becoming more pronounced closer to the surface, thus making U more mobile. The stable isotope (C and O) data seem to support post depositional alteration (Iyer et al., 1995). In the Sete Lagoas Formation organic C is present in varying amounts and the C isotope study

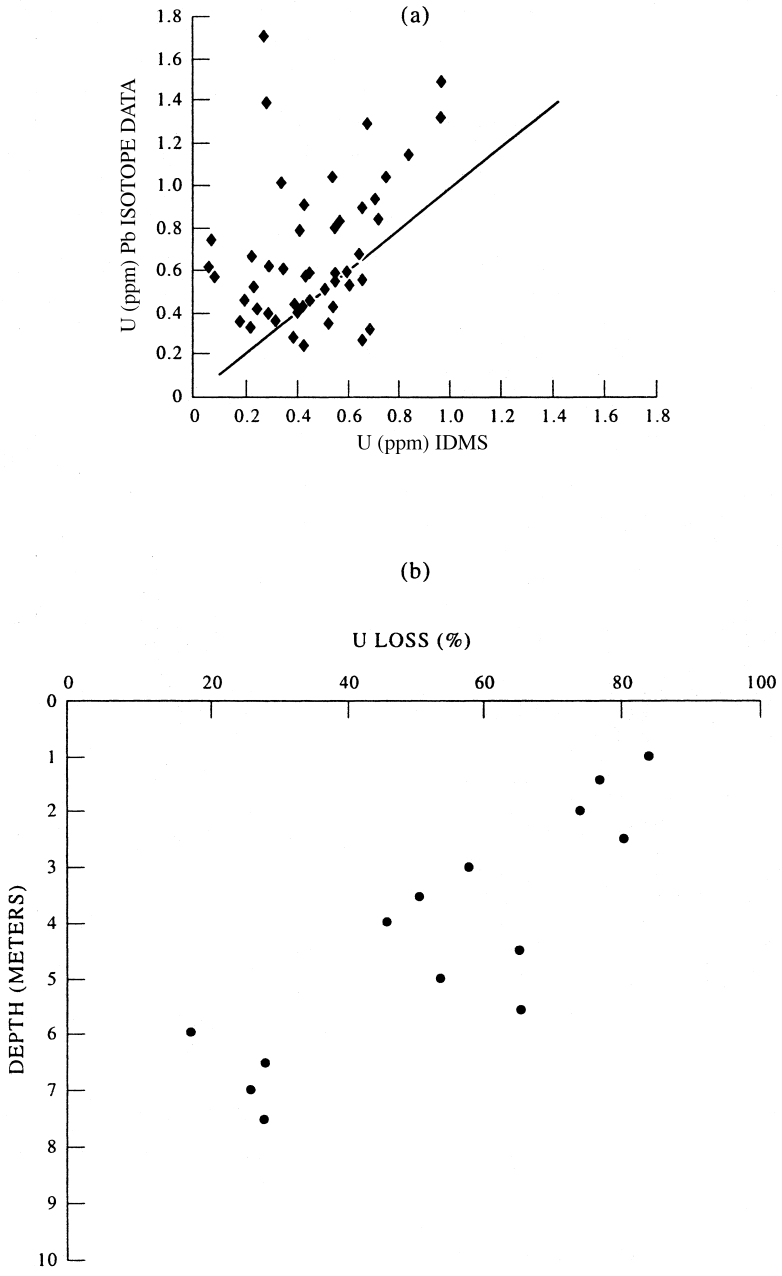

Fig. 3. Uranium loss in samples from the MF 7 outcrop. (a) Comparison of calculated (from Pb isotope data) and measured (mass spectrometric isotope dilution method) U contents. (b) Uranium loss (%) with depth (meters) below ground surface.

Table 3
Lead isotope data of carbonate rocks from the MF 10 outcrop, Bambui Group, Brazil (Babinski, 1993)

Sample number	$^{206}Pb/^{204}Pb$	$207Pb//^{204}Pb$	$^{208}Pb/^{204}Pb$	Pb(ppm)	U(ppm)	Th(ppm)	U(ppm)*	U Loss(%)
MF-10A1-L1	27.616	16.216	38.952	0.18	0.24	0.13	0.4	-69
MF-10A1-L2	32.276	16.473	38.614	0.23	0.41	0.13	0.35	15
MF-10A1-L3	34.103	16.511	38.288	0.49	0.96	0.23		
MF-10A2-L1	33.358	16.498	38.722					
MF-10A2-L2	41.412	17.037	38.877					
MF-10A2-L3	43.826	17.144	38.743					
MF-10A2-L4	43.561	17.183	38.9					
MF-10A3-WR	41.186	16.99	38.544	0.12	0.31	0.06	0.37	-21
MF-10A4-L2	52.91	17.596	38.671	0.1	0.34	0.05	0.38	-13
MF-10B1-L1	26.072	16.088	38.653	0.34	0.39	0.22	0.52	-33
MF-10B1-L2	27.706	16.216	38.689	0.59	0.78	0.37	0.51	35
MF-10B1-L3	28.37	16.196	38.486	0.69	0.97	0.39		
MF-10B2-L1	31.777	16.46	39.026					
MF-10B2-L2	36.327	16.698	39.143					
MF-10B2-L3	34.494	16.646	39.316					
MF-10B3-WR	35.393	16.648	39.132	0.38	0.78	0.27	0.37	53
MF-10B4-L2	36.842	16.777	39.361	0.34	0.74	0.26	0.52	30
MF-10C1-L1	25.822	16.148	38.863				0.57	
MF-10C1-L2	27.978	16.2	38.584				0.48	
MF-10C1-L3	29.496	16.369	38.819	0.26	0.39	0.17		
MF-10C3-WR	34.764	16.638	38.669	0.3	0.60	0.17	0.48	20
MF-10C4-L2	35.335	16.664	38.799	0.25	0.51	0.15	0.5	3
MF-10D1-L1	29.016	16.317	38.585	0.25	0.37	0.15	0.5	-37
MF-10D1-L2	28.87	16.3	38.502	0.2	0.29	0.11	0.42	-45
MF-10D1-L3	32.715	16.541	38.573	0.25	0.46	0.14		
MF-10D3-WR	34.999	16.714	38.701	0.42	0.85	0.25	0.43	50
MF-10D4-L2	44.885	17.247	38.886	0.19	0.53	0.11	0.46	14
MF-10E3-WR	36.139	16.666	38.969	0.14	0.30	0.09	0.49	-65
ME-10E4-L2	43.345	17.054	39.1	0.24	0.65	0.15	0.45	31
MF-10F3-WR	54.065	17.738	38.991	0.16	0.55	0.09	0.43	21
MF-10E4-L2	105.459	20.615	39.734	0.14	0.76	0.07	0.42	45
MF-10G1-L1	24.11	16.006	38.65	0.07	0.06	0.05		
MF-10G1-L3	27.718	16.204	38.539	0.16	0.21	0.09		
MF-10G2-L1	29.225	16.32	38.532	0.28	0.42	0.16		
MF-10G2-L2	32.353	16.518	38.94			0.00		
MF-10G3-WR	29.09	16.3	38.641	0.34	0.50	0.21	0.41	18
MF-10G4-L2	49.478	17.427	39.66	0.14	0.43	0.10	0.47	-8
MF-10H1-L2	55.813	17.872	39.699	0.14	0.49	0.10	0.48	2
MF-10H2-L2	54.62	17.808	39.712			0.00		
MF-10I1-L2	45.796	17.252	39.436	0.19	0.54	0.13	0.48	12
MF10J1-L2	32.782	16.502	39.345	0.37	0.67	0.29	0.54	20
MF-10K1-L2	61.68	18.129	39.472	0.17	0.65	0.10	0.63	3
MF-10L1-L2	45.777	17.234	38.869	0.16	0.46	0.09	0.47	-2
MF-10M1-L2	39.182	16.863	39.411	0.3	0.71	0.22	0.54	24
MF-10N1-L2	47.53	17.375	39.251	0.19	0.57	0.12	0.55	3
MF-10O1-L2	35.214	16.651	38.951	0.37	0.76	0.24	0.63	17

Average U (ppm) = 0.41 ± 0.3
Average Th (ppm) = 0.12 ± 0.08
* U measured by IDMS.

suggests near-equilibrium condition during the primary organic biosynthesis and carbonate formation in isotope equilibrium with CO_2 (Iyer et al., 1995). In the MF 7 profile the amount of organic C increases with depth (from 1% at the surface to 6% at 10 m below). The relation between the organic C content and the U retention at greater depth in MF 7 outcrop is far from clear. In this regard the suggestion of Nagy et al. (1993) about the graphite bitumen enclosing uraninite in the natural reactor at Oklo (serving as a protective medium around uraninite), inhibiting and preventing the loss of U and fission products is worth mentioning.

Compared to the MF 7 profile the amounts of organic C are much larger in Oklo, reaching up to 55% in a bitumen rich part of reactor zone (Levinthal et al., 1989). Lead–lead isotope dating and geochemical investigations on the organic matter may shed more light on this matter.

5.1.2. MF 10 outcrop

Twenty-five carbonate samples from this outcrop (Table 3) have been analyzed for their Pb isotope as well as U and Pb concentrations. The Pb isotope data of whole rock samples yields an isochron age of 520 ± 53 Ma (Fig. 4(a)). This age is much younger than the age for MF 7 samples, which are stratigraphically younger (situated at a higher level). This suggests that the Pb–Pb age of MF 10 outcrop represents a Pb isotope rehomogenization event during the final stages of the Brasiliano Orogeny. The U and Th values were calculated from the Pb isotope data considering this rehomogenization event (Fig. 4(a), (b)) and the values obtained are 0.41 ± 0.3 and 0.12 ± 0.08 ppm respectively (Fig. 4(c), (d)). A comparison of these calculated values with the measured U data (Fig. 5(a)) shows much lower loss of U in the MF 10 outcrop as compared to the MF 7 outcrop. Further, the lack of correlation of U loss with depth of sampling (Fig. 5(b)) suggests that the groundwater and/or oxidation conditions were probably similar throughout the MF 10 outcrop. The retention of much of the U in these samples is supported by the U–Pb isochron age of 600 Ma for the carbonates, where the U isotope data were calculated from isotope dilution measurement (Babinski, 1993). The isotope data for the MF 10 outcrop demonstrate that much of U can be retained for 600 Ma in sedimentary carbonates if the effects of post deposition alteration are minimum. In this outcrop the amount of coexisting organic carbon is similar throughout the profile (~2%).

5.1.3. MF 19 outcrop

This is the only outcrop sampled from the C_1 division (Fig. 1(b)) of Alkmim et al. (1989) and belongs to the Bambuí Basin's non-deformed domain. The outcrop belongs to the Sete Lagoas Formation, which is regionally known as Januária Formation (Dardenne, 1978). Outcrops consist of fine grained, medium to dark gray calcilutite and calcarenite with plane-parallel lamination showing signs of recrystallization. The analyzed samples in general contain fine grained calcite.

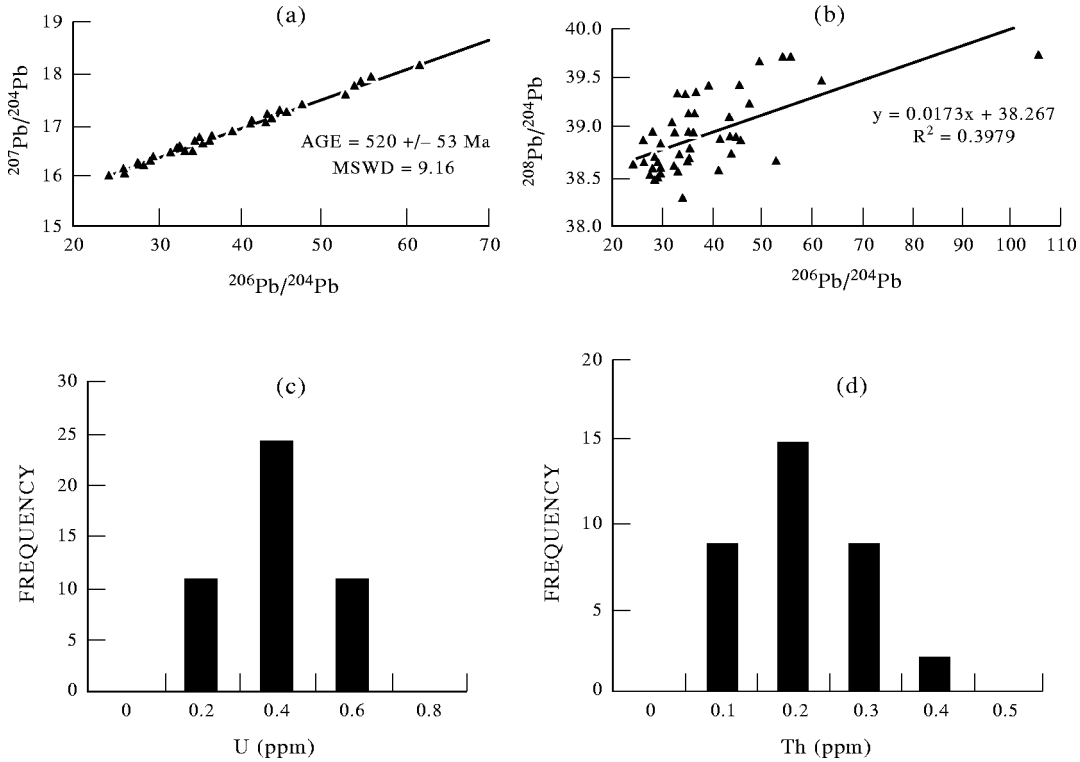

Fig. 4. Pb isotope systematics and U Th distribution in samples from the MF 10 outcrop (Babinski, 1993). (a) $^{207}Pb/^{204}Pb$ vs $^{206}Pb/^{204}Pb$ diagram showing age, μ_1 and MSWD values. (b) $^{208}Pb/^{204}Pb$ vs $^{206}Pb/^{204}Pb$ diagram. (c) Histogram of calculated U contents (ppm). (d) Histogram of calculated Th contents (ppm).

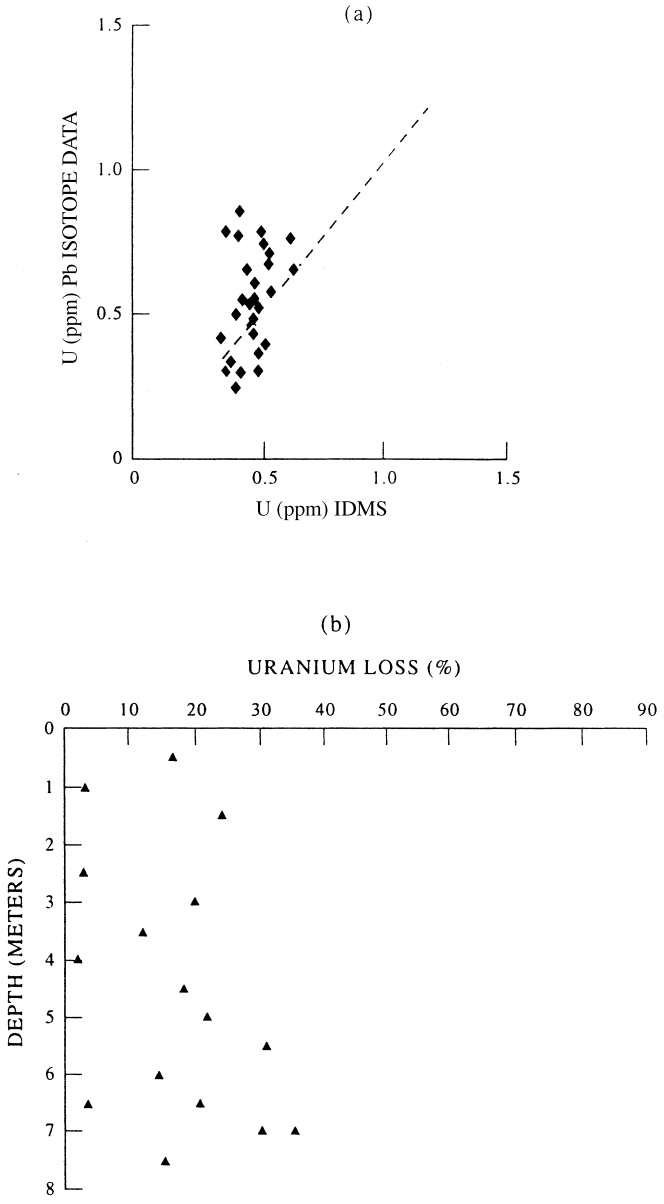

Fig. 5. Uranium loss in samples from the MF 10 outcrop. (a) Comparison of calculated (from Pb isotope data) and measured (mass spectrometric isotope dilution method) U contents. (b) Uranium loss (%) with depth (meters) below ground surface.

The samples show high radiogenic Pb isotope composition (Table 4 and Fig. 6(a), (b)) and the regression yields an isochron age of 565 ± 85 Ma. The age is interpreted to represent Pb isotope homogenization during the Brasiliano Orogeny. Uranium and Th concentrations calculated from the Pb isotope data show average values of 0.74 ± 0.24 and 0.16 ± 0.08 ppm respectively (Fig. 6(c), (d)). Uranium concentrations are much higher than those of samples taken from the MF 7 and MF 10 outcrops. Comparison of the MF 19 U values calculated from Pb isotope data with isotope dilution measurements shows that there have been large losses of U from all samples (Fig. 6(e)). One explanation may be that most of the minerals are very fine grained (< 0.004 μm) and may, as a consequence, be more susceptible to any minor alteration and dissolution than coarser grains in comparable rocks. These susceptible grains contain the bulk of the U and hence the U may be mobile. It should be pointed out that the alteration of these rocks may be related in the first instance to their physical properties of porosity and permeability (i.e. grain size), and secondly to the redox

Table 4
Lead isotope data of carbonate samples from MF 19 outcrop, Bambui Group, Brazil (Babinski, 1993)

Sample number	$^{206}Pb/^{204}Pb$	$207Pb/^{204}Pb$	$^{208}Pb/^{204}Pb$	Pb(ppm)	U (ppm)	Th (ppm)	U(ppm)*	U Loss (%)
MF-19A1-L2	41.951	17.148	39.61	0.39	1.22	0.35	0.61	50
MF-19A2-L2	42.62	17.176	39.594	0.39	1.24	0.35		
MF-19B1-L2	57.13	17.929	39.741	0.12	0.52	0.10	0.29	44
MF-19B2-L2	58.09	18.024	39.817	0.12	0.53	0.10		
MF-19C1-L2	51.253	17.706	39.34	0.2	0.78	0.15	0.38	52
MF-19D1-L2	74.362	19.072	39.23	0.17	0.91	0.10	0.61	33
MF-19D2-L2	80.895	19.416	39.176	0.17	0.97	0.09		
NF-19E1-L2	45.801	17.207	38.993	0.16	0.56	0.10	0.44	21
MF-19E2-L2	45.831	17.231	39.067	0.16	0.56	0.11		
MF-19F1-L2	61.605	18.323	40.155	0.14	0.65	0.13	0.34	47
MF-19F2-L2	57.458	18.002	39.803	0.14	0.61	0.12		
MF-19G1-L2	49.57	17.622	40.636	0.12	0.45	0.14	0.41	9
MF-19G2-L2	49.52	17.578	40.563	0.12	0.45	0.14	0.38	15
MF = 19-H1-L2	65.409	18.469	40.739	0.17	0.82	0.18	0.45	45
MF-19-H2-L2	62.944	18.421	40.788	0.17	0.79	0.19		
MF-19I1-L2	51.852	17.672	39.98	0.19	0.75	0.18	0.4	47
MF-19I2-L2	51.245	17.827	40.084	0.19	0.74	0.19		

Average U (ppm) = 0.74 ± 0.24
Average Th (ppm) = 0.16 ± 0.08
* U determination by IDMS.

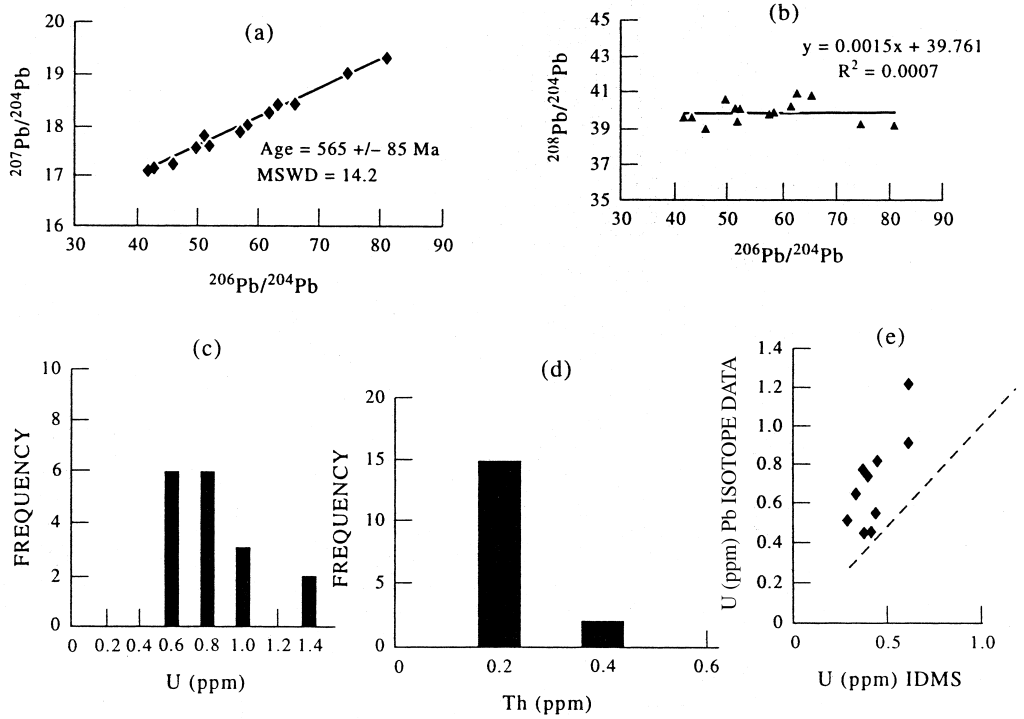

Fig. 6. Pb isotope systematics, U Th distribution and uranium loss in samples from the MF 19 outcrop (Babinski, 1993). (a) $^{207}Pb/^{204}Pb$ vs $^{206}Pb/^{204}Pb$ diagram showing age, μ_1 and MSWD values. (b) $^{208}Pb/^{204}Pb$ vs $^{206}Pb/^{204}Pb$ diagram. (c) Histogram of calculated U contents (ppm). (d) Histogram of calculated Th contents (ppm). (e) Comparison of calculated (from Pb isotope data) and measured (mass spectrometric isotope dilution method) U contents.

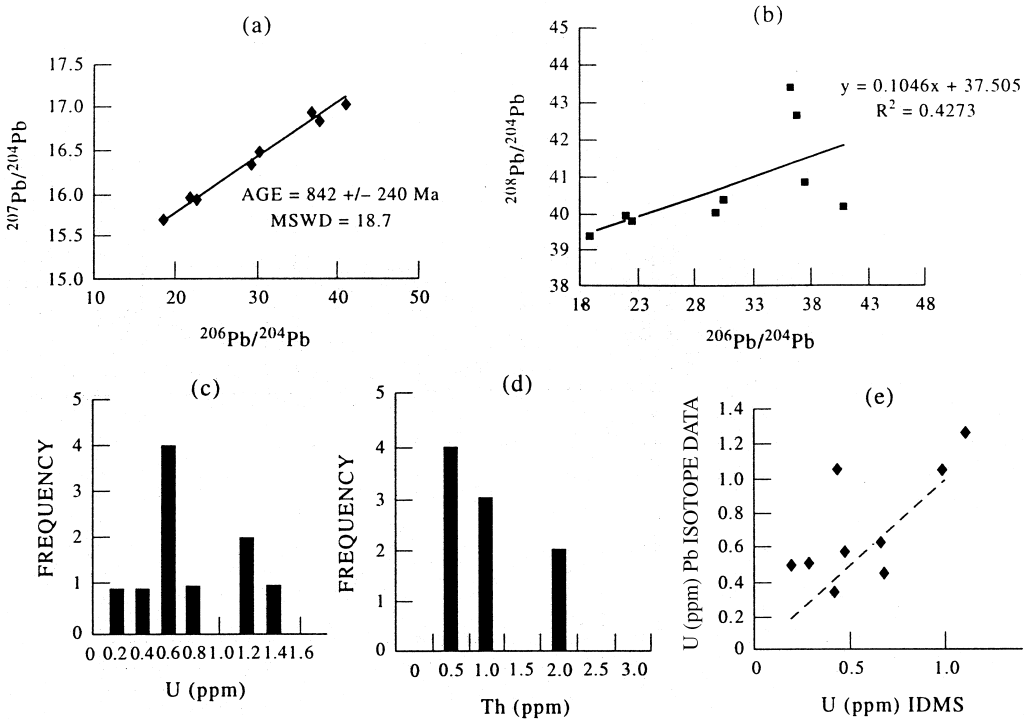

Fig. 7. Pb isotope systematics, U, Th distribution and uranium loss in samples from the MF 3 outcrop (Babinski, 1993). (a) $^{207}Pb/^{204}Pb$ vs $^{206}Pb/^{204}Pb$ diagram showing age, μ_1 and MSWD values. (b) $^{208}Pb/^{204}Pb$ vs $^{206}Pb/^{204}Pb$ diagram. (c) Histogram of calculated U contents (ppm). (d) Histogram of calculated Th contents (ppm). (e) Comparison of calculated (from Pb isotope data) and measured (mass spectrometric isotope dilution method) U contents.

conditions and composition of the ground water. The very fine grained size of the rocks probably had a greater influence in the U mobility.

5.1.4. MF 3 outcrop

This outcrop lies in the Eastern zone (E) where the strata are affected by both the W–E trending Araçuaí fold belt and deformation arising from the Brasiliano Orogeny. Rocks exposed in this outcrop belong to the Sete Lagoas Formation and are fine to medium grained, strongly recrystallized calcarenites. Light gray veins of calcite are also found in the outcrop and range in thickness from a few cm to 2m.

A plot (Fig. 7(a)) of the Pb–Pb isotope data of the samples (Table 5) yields an isochron age of 842 ± 240

Table 5
Lead isotope data of carbonate samples from MF 3 outcrop, Bambui Group, Brazil (Babinski, 1993)

Sample number	$^{206}Pb/^{204}Pb$	$207Pb/^{204}Pb$	$^{208}Pb/^{204}Pb$	Pb (ppm)	U(ppm)	Th(ppm)	U(ppm)*	U Loss (%)
MF-3A1-L1	18.912	15.685	39.405	1.98	0.50	1.55	0.19	62
MF-3A1-L2	19.034	15.682	39.423	3.9	1.04	3.07	0.44	58
MF-3B1-L1	22.137	15.936	39.876	0.88	0.51	0.79	0.29	43
MF-3B1-L2	22.518	15.932	39.856	2.03	1.25	1.80	1.10	12
MF-3C1-L1	29.592	16.344	40.043	0.15	0.18	0.13		
MF-3C1-L2	37.39	16.841	40.828	0.19	0.34	0.19	0.42	-24
MF-3D1-L2	36.773	16.911	42.583	0.61	1.04	0.89	0.99	5
MF-3E1-L1	36.425	16.904	43.317	0.38	0.64	0.63	0.67	-5
MF-3E1-L2	40.968	16.995	40.125	0.22	0.45	0.17	0.68	-52
MF-3F1-L1	30.304	16.448	40.338	0.45	0.58	0.42	0.47	19

Average U (ppm) = 0.65 ± 0.27
Average Th (ppm) = 0.96 ± 0.7
* U determined by IDMS.

Table 6
Lead isotope data of carbonate samples from the MF 9 outcrop, Bambui Group, Brazil (Babinski, 1993)

Sample number	$^{206}Pb/^{204}Pb$	$207Pb/^{204}Pb$	$^{208}Pb/^{204}Pb$	Pb(ppm)	U (ppm)	Th (ppm)	U(ppm)*	U Loss (%)
MF-9A1-L2	23.476	16.008	39.027	0.75	0.59	0.54	0.66	-12
MF-9B1-L2	20.643	15.818	38.827	2.37	1.25	1.62	0.69	45
MF-9C1-L2	21.624	15.888	38.82	1.75	1.09	1.18	0.52	52
MF-9D1-L1	20.638	15.831	38.81	1.89	1.00	1.28	0.14	86
MF-9D1-L2	20.782	15.817	38.765	1.73	0.94	1.15	0.73	22
MF-9E1-L1	20.741	15.839	38.873	1.54	0.83	1.07	0.07	92
MF-9E1-L2	21.165	15.849	38.909	1.83	1.06	1.29	0.32	70
MF-9F1-L1	21.589	15.899	38.982	0.57	0.35	0.41	0.05	86
MF-9F1-L2	21.994	15.898	38.886	1.36	0.89	0.94	0.4	55
MF-9G1-L2	32.619	16.446	38.904	0.34	0.52	0.21	0.54	-4

Average U (ppm) = 0.85 ± 0.28
Average Th (ppm) = 0.97 ± 0.45
* U determined by IDMS.

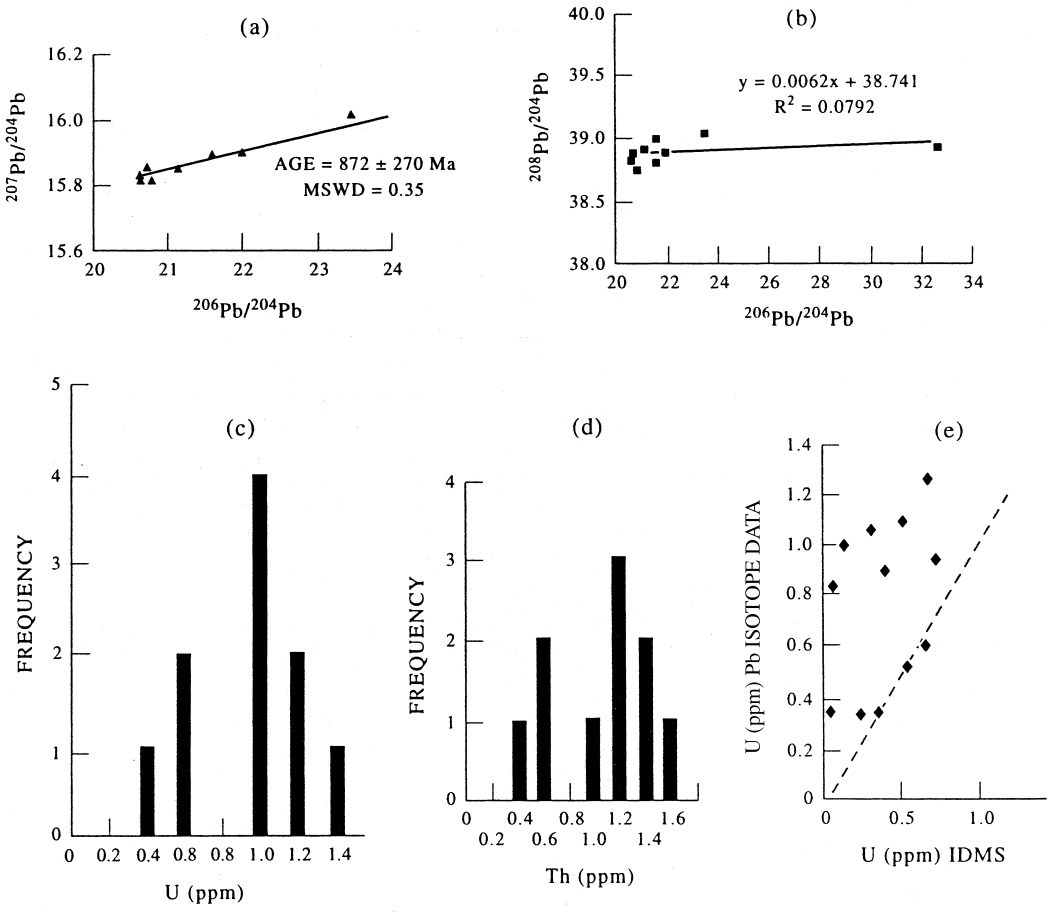

Fig. 8. Pb isotope systematics and U Th distribution and uranium loss in samples from the MF 9 outcrop (Babinski, 1993). (a) $^{207}Pb/^{204}Pb$ vs $^{206}Pb/^{204}Pb$ diagram showing age, μ_1 and MSWD values. (b) $^{208}Pb/^{204}Pb$ vs $^{206}Pb/^{204}Pb$ diagram. (c) Histogram of calculated U contents (ppm). (d) Histogram of calculated Th contents (ppm). (e) Comparison of calculated (from Pb isotope data) and measured (mass spectrometric isotope dilution method) U contents.

Ma. The large error of 240 Ma is due to the limited number of samples analyzed and the small spread in the data (Fig. 7(a)). Uranium and Th concentrations calculated from the isotope data (Fig. 7(a), (b)) yield average values of 0.65 ± 0.27 ppm and 0.96 ± 0.7 ppm respectively (Fig. 7(c), (d)). Comparison of the U values calculated from Pb isotope data with analyzed U contents for these samples reveal that there has been some loss of U (Fig. 7(e)). The MF 3 outcrop occupies the same stratigraphic position as that of MF 19 for which there has been a recent large loss of U. Unlike the case of MF 19 samples the U loss in the MF 3 outcrops may be related more to the redox conditions and composition of the ground water than to the physical properties of the samples, as they are fine to medium grained.

5.1.5. MF 9 outcrop

Deformed dark gray dolomites from the western part (W) of the Bambuí basin have been analyzed for their Pb isotope composition (Table 6). In thin section the dolomite and calcite crystals are seen to be strongly recrystallized, with both grain boundaries straight and sutured. Well crystallized calcite veins (thickness of 0.01 mm) are very common in these rocks.

Lead isotope data of 7 samples (Fig. 8(a)) yield an isochron age of 872 ± 270 Ma. The large error of 270 Ma is partially due to the smaller number of analyses. The outcrop is located within a zone of intense deformation arising from the Brasiliano Orogeny. Because this Orogeny probably reset the Pb isotopes in the analyzed samples, the 872 Ma value is considered to be an apparent minimum age. Uranium and Th contents calculated from the Pb isotope data (Fig. 8(a), (b)) have average values of 0.85 ± 0.28 and 0.97 ± 0.45 ppm respectively (Fig. 8(c), (d)). The U loss (Fig. 8(e)) appears to be moderate to high and may be due to the different intensities of meteoritic alteration which was demonstrated to have occurred by Iyer et al.(1995), who studied $\delta^{13}C$ and $\delta^{18}O$ variations in the samples of the outcrop.

Studies of 5 outcrops (MF 7, MF 10, MF 19, MF 9, MF 3) of the Neoproterozoic carbonates have revealed systematic recent U loss in some outcrops and U retention in others. The observations indicate that the mobility of U is due to alteration by meteoric waters. In at least one outcrop (MF 7) a clear correlation between U loss and depth of sampling suggests that the influence of groundwater was greater near the top of the vertical profile and is supported by stable isotope data for C and O. The possible role of the organic C in the retention of U in the MF 7 outcrop needs to be further investigated.

Table 7
Lead isotope data of calc-alkaline volcanic rocks interbedded with the Mirante Formation, Contendas–Mirante Complex, Brazil (Marinho, 1991)

Sample number	$^{206}Pb/^{204}Pb$	$207Pb/^{204}Pb$	$^{208}Pb/^{204}Pb$	Pb(ppm)	U (ppm)	Th (ppm)	U(ppm)*	Th(ppm)*	U Loss(%)	Th Loss(%)
MM25A	30.639	18.017	46.826	14.2	5.72	16.10	4.25	15.9	26	1
MM27	28.898	17.7	45.072	21.8	8.14	22.23	4.82	18.9	41	15
MM28B	24.504	17.007	41.549							
MM24	38.666	19.037	53.03							
MM39	25.904	19.933	42.023	12	3.69	9.26	0.3	6.3	92	32
MM98	19.619	15.934	39.437	21	3.31	12.87	4.4	13.8	-33	-7
MM151B	19.211	15.869	39.056	8.5	1.24	4.90	0.3	4.1	76	16
MM151C	19.562	15.897	40.485	6.2	0.95	4.47	0.63	3.4	34	24
MM152C	21.562	16.247	42.816	6.7	1.37	6.18	0.3	4.7	78	24
MM158B	41.712	19.6	54.858	10.2	5.74	15.48	4.76	14.55	17	6

AvU (ppm) = 3.66 ± 2.5
Av Th (ppm) = 11.44 ± 6.32
* Measurement by XRF.

5.2. Contendas–Mirante Complex

Extensive geochronological investigations using different isotopic clocks have been carried out on different rock formations in this Archean/Proterozoic terrain (Marinho, 1991; Marinho et al., 1995). The geochronological data for rock units of the Contendas–Mirante volcanic–sedimentary belt suggest a crustal evolutionary history ranging from 3.5 Ga to 2.0 Ga with major events at 3.5 Ga, 3.0 Ga, 2.5 Ga and 2.0–1.8 Ga, respectively. Two of the units from this complex have been selected for the present study: the calc–alkaline volcanics of the Mirante Formation, and the Pé de Serra granite. These units have been chosen in the framework of site selection procedure of Brazilian waste disposal, as the volcanic rocks and granites are considered to be suitable host rocks for high level radioactive waste in the USA, Canada, and Sweden. The data for these two units are discussed below.

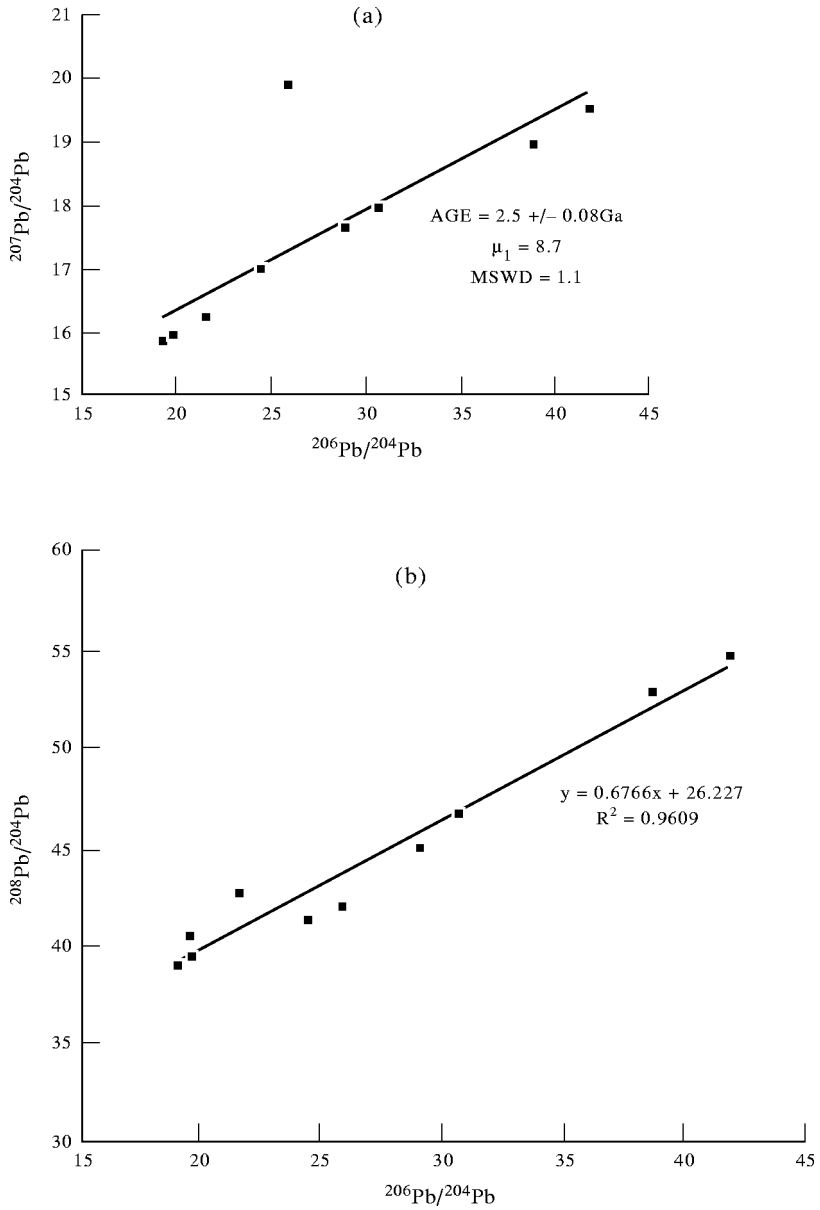

Fig. 9. Pb isotope systematics in samples from calc volcanic rocks, Contendas–Mirante Complex (Marinho, 1991). (a) $^{207}Pb/^{204}Pb$ vs $^{206}Pb/^{204}Pb$ diagram showing age, μ_1 and MSWD values. (b) $^{208}Pb/^{204}Pb$ vs $^{206}Pb/^{204}Pb$ diagram.

5.2.1. Calc–alkaline volcanic rocks

Marinho (1991) carried out Pb–Pb dating of calc–alkaline volcanic rocks included within the Mirante formation. Regression of the isotopic data (Table 7) yields two approximately parallel alignments (Fig. 9(a)) giving concordant ages of 2.49 ± 0.081 Ga ($\mu_1 = 8.8$) and 2.519 ± 0.016 Ga ($\mu_1 = 8.1$) The volcanic rocks are therefore considered to be about 2.5 Ga old. The calculated U and Th values from the Pb isotope data (Table 7; Fig. 9(a), (b)) show a large spread with average values of 3.7 ± 2.5 and 11.4 ± 6.3 ppm respectively (Fig. 10(a), (b)). The large spread of values may be due to the volcanics being derived from a range of parental materials differing significantly in composition. A comparison of the U and Th concentrations calculated from the Pb isotope data with measured values shows a large recent loss of U, whereas Th appears to have been retained in the rocks (Fig. 10(c), (d)). Though it is believed that most of the U and Th are held in the accessory minerals like zircon, apatite, some U may be loosely held within fractures and, grain boundaries and thus is susceptible to being mobilized by groundwater under oxidizing conditions. Whole rock data for these rocks (Marinho, 1991) show a good inverse correlation between the U loss and $FeO/(FeO + Fe_2O_3)$, i.e. generally the higher the oxidation ratio the greater the U loss.

5.2.2. Pé de Serra granite

A major intrusive body in the Contendas–Mirante belt is the Pé de Serra granite, which occupies an area of about 500 km^2. Geochronolgical data for this amphibole bearing sub-alkaline granite (Marinho, 1991) show a Pb–Pb isochron age of 2.56 ± 0.11 Ga (Table 8, Fig. 11(a)) which is considered to be the time of intrusion. From the Pb isotope data (Fig. 11(a), (b)) the U and Th values are calculated (Table 8, Fig. 12(a), (b)). The radioactive element concentrations and radiogenic heat production value of this granite are similar to those obtained by Bunker et al. (1975) for Archean granites from Western Australia and are higher than those of other rock units in the Contendas–Mirante

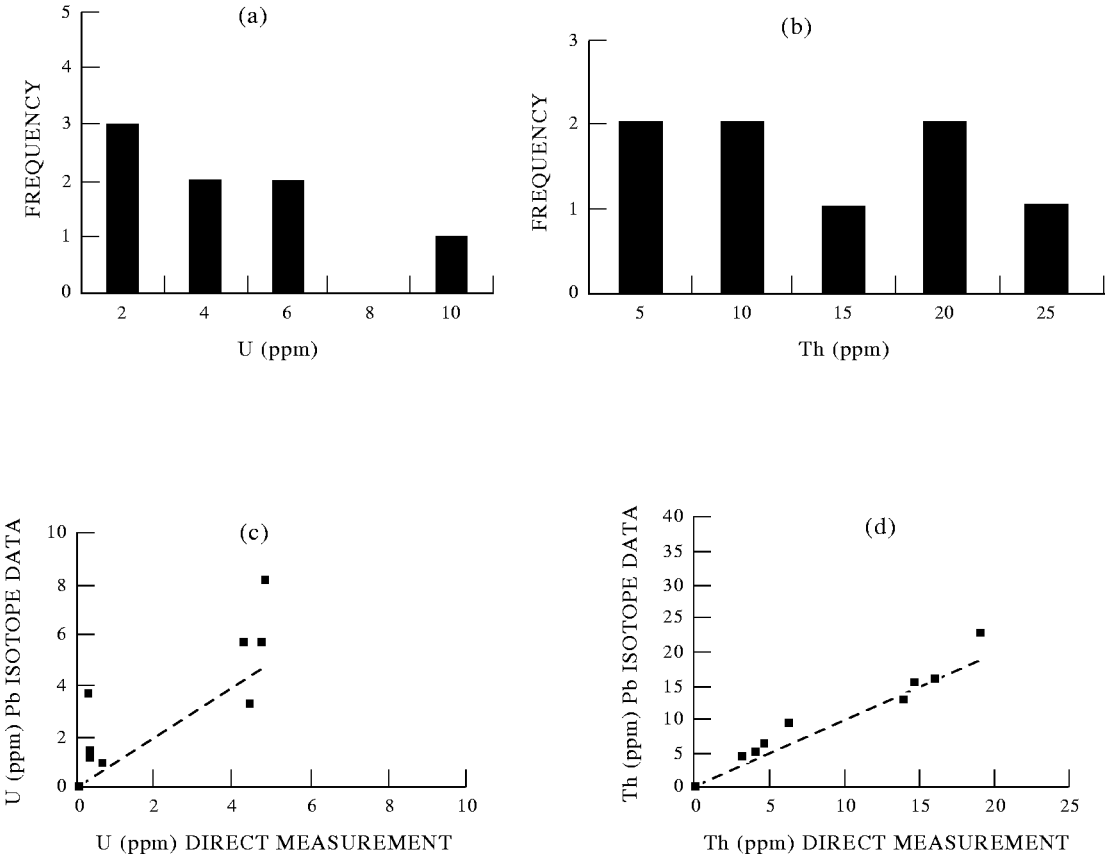

Fig. 10. U Th distribution in calc volcanic rocks, Contendas–Mirante Complex. (a) Histogram of calculated U contents (ppm). (b) Histogram of calculated Th contents (ppm). (c) Comparison of calculated (from Pb isotope data) and measured (X ray fluorescence method) U contents. (d) Comparison of measured and calculated Th contents.

Table 8
Lead isotope data of the Pé de Serra granite, Contendas–Mirante Complex, Brazil (Marinho, 1991)

Sample number	$^{206}Pb/^{204}Pb$	$207Pb/^{204}Pb$	$^{208}Pb/^{204}Pb$	Pb (ppm)	U (ppm)	Th (ppm)	U(ppm)*	Th(ppm)*	U Loss (%)	Th Loss (%)
MM30A	18.161	15.741	37.305	76	10.3	39.1	13	23	-26	41
MM30C	18.791	15.908	38.131	44.2	6.8	26.3	10.1	22.2	-49	16
MM30D	18.761	15.968	38.06	74	11.2	43.5	12		-7	
MM30E	19.629	16.028	38.824	35.5	6.2	23.4	5.7	21.1	9	10
MM31	18.592	15.873	37.801	37.5	5.5	21.1	4.1	17.6	26	17
MM32A	20.774	16.259	40.127	58	11.9	44.9	6		49	
MM32B	22.489	16.545	42.085	34.3	8.4	32.1	8.8	32.2	-5	-0
MM160A	22.69	16.541	42.368	35.6	8.9	34.1	7.9	33.9	11	1
MM160B	20.629	16.217	40.274	35	7.0	27.7	8.2	25.3	-17	9
MM160C	20.845	16.279	40.461	62	12.7	49.9				
MM132	23.361	16.348	39.582	6.7	1.8	4.7	0.3	4.6	84	2
MM163	28.738	17.132	52.288	10.2	3.6	16.6	4.1	24.2	-14	-46
MM163BIS	28.44	17.074	51.763							

Av. U (ppm) = 7.9 ± 2.7
Av.Th (ppm) = 30.2 ± 10.3
* measurement by XRF.

Complex. This is mainly due to the higher concentrations of accessory minerals such as zircon, apatite and monazite.

A comparison of the calculated U and Th concentrations based on Pb isotope data with measured values of these elements (Fig. 12(c), (d)) reveal that there has been little, if any, loss of these two elements from the analyzed granite samples, probably because they are strongly held within the crystal lattice. Geoechemical data for this granite (Marinho, 1991) show uniform chemical composition with the FeO/($FeO + Fe_2O_3$) ratios within a narrow range. The Th and U concentrations are well correlated (Fig. 11(c)) and the average Th/U ratio of about 4 agrees well with the values normally observed in plutonic rocks (Marinho, 1991). Marinho (1991) found that the rare earth element pattern in the granite is strongly fractionated with a negative Eu anomaly, thus indicating that the granite has maintained its original magmatic chemical composition. Factors that encourage the mobilization of radioactive elements, such as the presence of fracture zones, oxidation and large-scale fluid circulation (Menager et al., 1992) are either insignificant or absent in this granite. Because of its ability to retain the radioactive elements, this granite may potentially be a better site than the calc–alkaline rock for a Brazilian radioactive waste repository. Further studies on the granite's petrography, geochemistry and oxygen isotopes are currently in progress.

5.2.3. Lagoa real granite–ortho-gneiss complex

Lead isotope data for 7 samples of undeformed granite and for 8 samples of granitic ortho-gneisses belonging to this Complex (Table 9), are plotted in a $^{207}Pb/^{204}Pb$–$^{206}Pb/^{204}Pb$ isochron diagram in Fig. 13(a). Most of the samples define a well fitted isochron with a calculated age of 1.7 ± 0.1 Ga and an apparent m_1 value of 8.86. The samples which do not conform well to this isochron (one granite and two ortho-gneisses) may have been subjected to an influx of U during the formation of some nearby albitites (Cordani et al., 1992). The overlap of the Pb-isotope compositions of the granites and ortho-gneisses is consistent with the interpretation that the ortho-gneisses are deformed equivalents of granites and their common Pb-isotope growth was not disturbed by gneissification. The Pb–Pb age appears concordant with the U–Pb zircon age of 1.725 ± 0.005 Ga obtained by Turpin et al. (1988) for non-deformed, partially recrystallized granites and deformed ortho-gneisses. According to Turpin et al. (1988) gneissification did not affect the composition of the zircons, except for metamict and small zircons which record a much younger event of 500 Ma. The available Pb–Pb isotope data are a good indication that the isotope system remained closed

since the formation of the granite. This is in direct contrast to the open behavior of Rb–Sr (Cordani et al., 1992) and Sm–Nd (Turpin et al., 1988) systems, demonstrating the reliability of the Pb–Pb isotope clock in preserving early isotopic equilibria in polymetamorphic terrains.

From the Pb isotope data (Fig. 13(a), (b)) the concentrations of present day U and Th are calculated and are compared with the U and Th values in the same samples measured by the X-ray Fluorescence technique (Table 9). This comparison clearly demonstrates a large loss (70 to 90%) of U and a moderate to low loss of Th (Fig. 13(c), (d)). The analyzed orthogneiss samples are unweathered, and are obtained from drill cores in zone of U mineralization. They are from a depth of 50 to 110 m below the surface. All samples show a similar calculated loss of U, suggesting that conditions favorable for recent U mobility persisted up to depths of 100 m or more.

Maruejol et al. (1987) carried out a systematic geochemical study of the Lagoa Real Complex and observed a large variation in Th contents (5 to 76 ppm), whereas the U contents were more limited in range. Th/U ratios were found to vary from 4 to 10 similar to most altered granites and this variation was attributed to the probable preferential loss of U over Th from metamict secondary minerals (e.g. allanite, Nb ± Ti REE minerals) through the preferential leaching of U. These observations agree with the present day U, Th concentrations analyzed by Maruejol et al. (1987) suggesting that the U depletion is a recent phenomenon.

In his discussion on fluid infiltration in fault zones Kerrich (1986a); Kerrich, 1986b) cites Lagoa Real as a good example of fluid flow in a brittle-ductile shear zone stating that U mobilization and deposition were facilitated by fluid flow during the overthrusting of the basement rocks over the sediments. As mentioned earlier, data on the geochemistry (Maruejol et al., 1987) fluid inclusions (Fuzikawa et al., 1988) and geochronology (Turpin et al., 1988; Cordani et al., 1992) do not support the mobilization of U from the rock

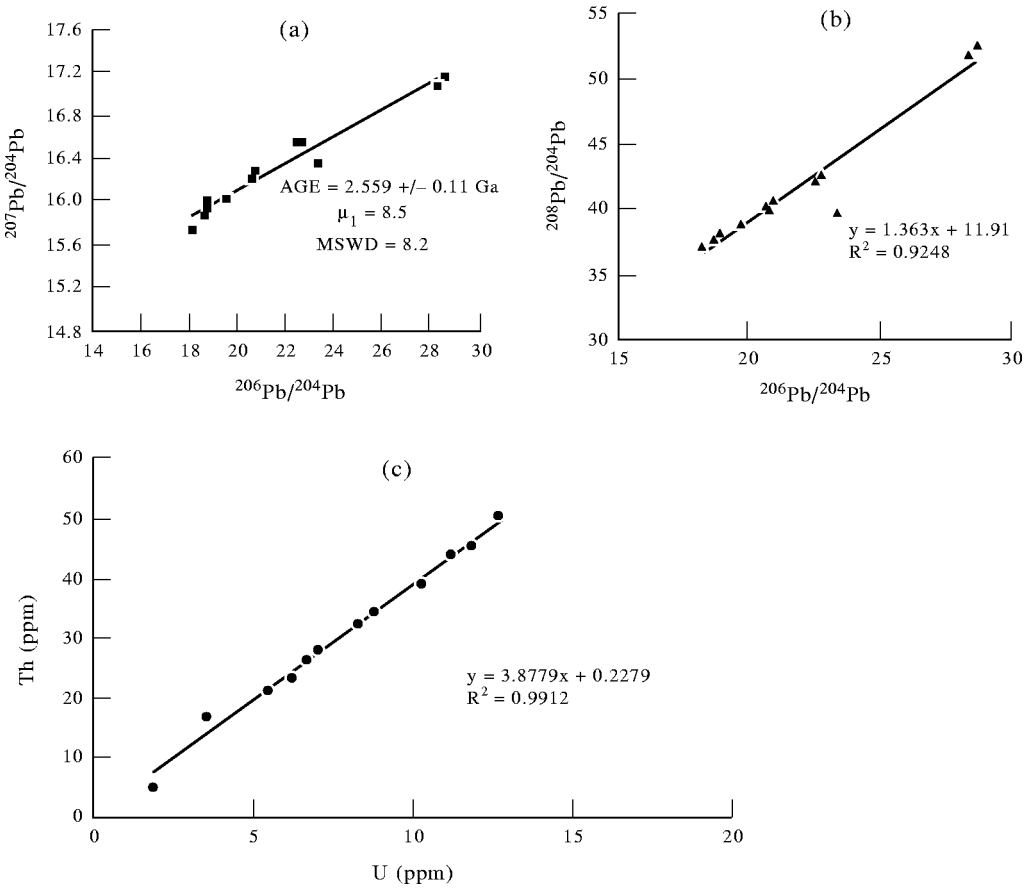

Fig. 11. Pb isotope systematics in samples from the Pé de Serra Granite. Contendas–Mirante Complex (Marinho, 1991). (a) $^{207}Pb/^{204}Pb$ vs $^{206}Pb/^{204}Pb$ diagram showing age, μ_1 and MSWD values. (b) $^{208}Pb/^{204}Pb$ vs $^{206}Pb/^{204}Pb$ diagram. (c) U versus Th diagram.

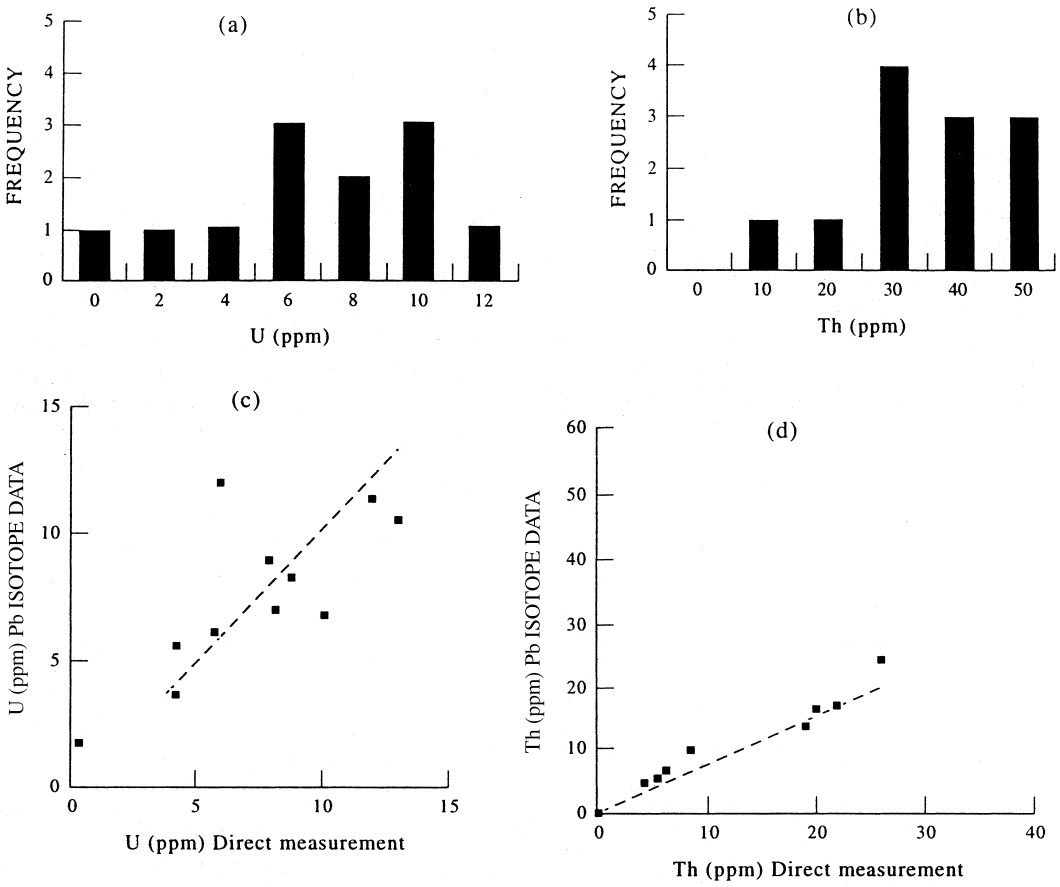

Fig. 12. U Th distribution in the Pé de Serra Granite, Contendas–Mirante Complex. (a) Histogram of calculated U contents (ppm). (b) Histogram of calculated Th contents)ppm). (c) Comparison of calculated (from Pb isotope data) and measured (X ray fluorescence method) U contents. (d) Comparison of measured and calculated Th contents.

during the overthrusting event, but point to a probable redistribution of U with probably a minimal fluid activity. However it is possible that the shear zones in the granite ortho-gneisses served as conduits for groundwater activity in recent times thus facilitating loss of U, and to a lesser degree, Th from the rocks. Lobato and Fyfe (1990) observed a progressive increase in the oxidation of mineral phases accompanied by Na enrichment in gneisses with height in and along the shear zones, and a good correlation of U enrichment with Fe_2O_3.The samples analyzed in the present study have similar $FeO/(FeO + Fe_2O_3)$ ratios and similar large U loss.

The Lagoa Real Complex may be considered for natural analogue studies related to disposal of high level radioactive waste in granitic rocks. Several economic and sub-economic U deposits exist in the Lagoa Real Complex with the main U bearing mineral being uraninite.

6. Conclusions

This study demonstrates the usefulness of isotopes to determine quantitatively the mobility of U and Th in different geological environments. The isotope data indicate that large scale mobility of U occurred in the studied carbonate sedimentary rocks and deformed ortho-gneisses, the latter being cut by a ductile shear zone which hosts an economic uranium deposit. In comparison, the undeformed calc–alkaline volcanics and granitic rocks retained much of their U and Th. The study indicates a larger U mobility in near surface and oxidizing conditions. The suitability of geological sites for disposal of radioactive waste is essentially linked to the retention capacity of the site for the radioactive elements and the study of analogue formations provide basic guidelines for a better understanding of elemental migration processes (Ménager et al., 1992). Geochemical data are needed to assess the

Table 9
Lead isotope data of granites and granitic gneisses, Lagoa Real Complex, Brazil (Cordani et al., 1992)

Sample number	$^{206}Pb/^{204}Pb$	$207Pb/^{204}Pb$	$^{208}Pb/^{204}Pb$	Pb (ppm)	U(ppm)*	Th(ppm)*	U(ppm)	Th(ppm)	U Loss (%)	Th Loss (%)
PE WB 22A	18.801	15.798	41.462							
QE-WB-28.1	18.112	15.715	39.813							
PEML 697-3	24.749	16.573	53.702							
LR 16 B	17.951	15.713	43.295							
LR 17 A	17.163	15.624	39.025							
GA 286B	18.485	15.764	42.08							
GA 798	19.224	15.735	43.58							
FEN-01(54.50)	22.009	16.134	42.256	25.3	3.3	16.8	16.3	31.9	80	47
FEN-01(79.75)	21.527	16.076	43.932	24.3	2.1	29	14.8	45.8	86	37
FCA-03(88.25)	19.594	15.881	40.944	20	1.7	14.8	8.9	17.1	81	13
FCA-15(97.5)	18.603	15.748	40.935	25.2	2.8	19.5	8.8	22.1	68	12
FEN-01(81.75)	20.688	15.998	45.342	22	3.5	25.9	11.8	53.9	70	52
FEN-01(83.5)	34.234	17.533	50.741							
FCA-13(66.5)	18.475	15.781	40.727	15.6	<1	19.2	5.3	12.5		-54
FCA-10(116.25)	17.984	15.718	39.734	22.2	<1	12.2	6.4	9.2		-33

Av. U (ppm) = 10.3 ± 3.4
Av. Th (ppm) = 27.5 ± 14
* Measurement by XRF.

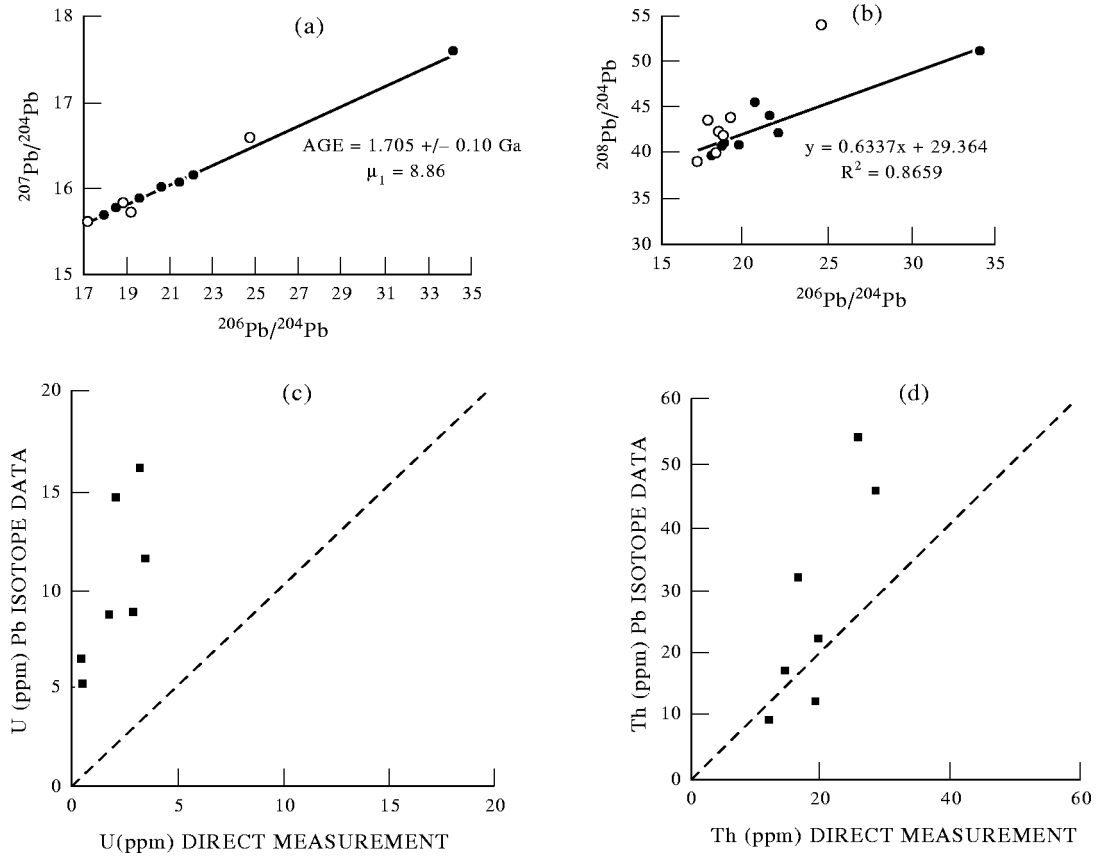

Fig. 13. Pb isotope systematics in granites and ortho-gneisses from the Lagoa Real Complex (Cordani et al., 1992). (a) $^{207}Pb/^{204}Pb$ vs $^{206}Pb/^{204}Pb$ diagram showing age, μ_1 and MSWD values. (b) $^{208}Pb/^{204}Pb$ vs $^{206}Pb/^{204}Pb$ diagram. (c) Comparison of calculated (from Pb isotope data) and measured (X ray fluorescence method) U contents. (d) Comparison of measured and calculated Th contents.

suitability of proposed sites and the Pb isotope approach may be very useful for site selection. The Pé de Serra granite appears to be a suitable candidate for Brazilian radioactive waste disposal site.

In conclusion, the main point emphasized by the present study is the use of Pb isotopes in studying the mobility of radioactive elements in various rocks. The Pb isotope approach may be considered a complementary method to U series disequilibrium studies.Barbosa and Dominguez, 1996

Acknowledgements

The present study benefited from discussion with many of our colleagues. Special mention should be made of John Ross, Don Russell, Umberto Cordani, Jorma Heinonen and Stan Hallas for their encouraging comments. Critical reviews of two anonymous referees and useful suggestions of J. C. Petit on an earlier draft helped improve many ideas expressed in this manuscript. Marly Babinski thanks Conselho Nacional de Desenvolvimento Cientifico e Technologico (CNPq Proc. No. 20.3157/89.3) and I. M. Sato acknowledges the financial support of PADCT/CNPq.

Appendix A. The lead isotope approach to estimating the upper limit for the date of uranium mobility in a rock system

Although the Pb isotope method cannot be used to determine the date of U mobility in a rock system, a rough estimate of an upper limit to the date of that mobility may be ascertained, as shown below.

It is assumed here that the U–Th–Pb isotope system of a rock sample remains closed from time "t" until today ($t = 0$). In this case the Pb isotope evolution

may be described as:

$$(^{206}Pb/^{204}Pb)_a - (^{206}Pb/^{204}Pb)_i = \mu_2[e^{\lambda t} - 1] \quad (A1)$$

Suppose this rock sample lost or gained U at time "t_1" (single episode loss) and the μ_2 value changed to μ_3, then the above equation may be rewritten as:

$$(^{206}Pb/^{204}Pb)_b - (^{206}Pb/^{204}Pb)_i = \mu_2(e^{\lambda t} - e^{\lambda t1}) + \mu_3(e^{\lambda t1} - 1) \quad (A2)$$

Subtracting Eq. (A2) from Eq. (A1), we obtain:

$$(^{206}Pb/^{204}Pb)_a - (^{206}Pb/^{204}Pb)_b = (\mu_2 - \mu_3)(e^{\lambda t1} - 1) \quad (A3)$$

Eq. (A3) shows that the change in Pb isotope composition between the closed system without any loss or gain of U and the same system with a recent mobility is dependent on the time of mobility and the change in μ value (amount of loss or gain of U).

Assuming a hypothetical case of a sample with (μ_2–μ_3) = 10 and $t_1 = 50$ Ma then from Eq. (A3)

$$(^{206}Pb/^{204}Pb)_a - -(^{206}Pb/^{204}Pb)_b = 0.07$$

This value is generally close to the lower accuracy limit in the analytical measurement of Pb isotope and lies within the error limit of the isochron date (Babinski, 1993). Thus 50 Ma may be considered an upper limit for the date of U mobility. It may be mentioned that a large loss of U has been assumed in this calculation. The time span covered is related to the amount of U loss; the higher the loss, the lower is the upper limit for the time period of the loss.

Appendix B. Calculation procedure for U and Th from lead isotope data

The Calculation procedure is illustrated with an example from the Pe de Serra granite.

The general parameters:

T = age of the earth = 4.57 Ga;

$\lambda(^{238}U) = 0.155125 \times 10^{-9}$ yr^{-1};

$\lambda'(^{235}U) = 0.98485 \times 10^{-9}$ yr^{-1};

$\lambda''(^{232}Th) = 0.049475 \times 10^{-9}$ yr^{-1},
$(^{206}Pb/^{204}Pb)pr = 9.307$;
$(^{207}Pb/^{204}Pb)pr = 10.294$; $(^{208}Pb/^{204}Pb)pr = 29$.

Data from Pe de Serra granite

$t = 2.56$ Ga; $\mu_1 = 8.5$; $\kappa_1 = 28.4$

Sample MM 30A (Table 8)

Substituting the values of "t" and μ_1 in Eq. (4), we obtain

$(^{206}Pb/^{204}Pb)_i = 13.93$

Substituting the value of "t" and κ_1 in an equation for thorogenic lead, we obtain

$(^{208}Pb/^{204}Pb)_i = 32.37$

From Eqs. (1) and (3) the present day μ_2 ($^{238}U/^{204}Pb$) = 8.67 and κ_2 ($^{232}Th/^{204}Pb$) = 33.15 are obtained.

Pb concentration in MM 30A = 76 ppm and ^{204}Pb (nmoles/g) = 5.079

Hence ^{238}U (nmoles/g) = 44.05 ^{232}Th (nmoles/g) = 168.37

U (ppm) = 10.5; Th(ppm) = 39.1

References

Adams, J. A. S., Weaver, C. D., 1958. Thorium to uranium ratios as indicators of sedimentation processes: example of the concept of geochemical facies. Bull. AAPG 42, 416–430.

Ahearne, J. F., 1997. Radioactive waste: the size of the problem. Physics Today 50, 24–29.

Alkmim F. F., Chemale F., Bacellar L. A. P., Magalhares P. M., 1989. Arcabouço estrutural da porção sul do Bacia do São Francisco. 5th Symp. Geologia do Nucleo Minas Gerais, pp. 289–293.

Almeida, F. F. M., 1977. O Craton do São Francisco. Rev. Bras. Geoc. 7, 349–364.

Babinski M. 1993. Idades isocronicas Pb/Pb e geoquimica isotopica de Pb das rochas carbonaticas do Grupo Bambuí no porção sul de bacia do São Francisco. Unpubl. Ph.D. dissertation, Universidade de São Paulo, Brazil.

Barbosa J. S. F., Dominguez J. M. L., 1996. Texto Explicativo sobre a mapa Geologica Milinésimo. SICH/SGM. UFBA, Salvador.

Bayer G., Rogers J. J. W., Adams J. A. S. and Haack U. K., 1978. Thorium. In Wedepohl, K. H. (ed) Handbook of Geochemistry. Springer-Verlag, Berlin.

Bonhomme, M. G., 1976. Mineralogie des fractions et datations rubidium strontium dans le Groupe Bambuí, MG, Bresil. Rev. Bras. Geoc. 6, 211–220.

Bonhomme, M. G., Cordani, U. G., Kawashita, K., Macedo, M. H. F., Thomaz Filho, A., 1982. Radiochronological age and correlation of Proterozoic sediments in Brazil. Precamb. Res. 18, 103–118.

Bunker C. M., Bush M. R. I., Sass J. H., 1975. Abundances of uranium, thorium and potassium for some Australian crystalline rocks. USGS Open File Report 75-383.

Chapman N. A., Smellie J. A. T., 1986. Introduction and summary of the workshop. In Chapman, N. A., Smellie, J. A. T. (Eds) Natural analogues to the conditions around a final repository for high level radioactive waste. Chem. Geol., Vol. 55, pp. 167–173.

Chemale F., Alkmim F. F., Endo I., 1993. Late Proterozoic tectonism in the interior of the São Francisco Craton. In Findlay, R. H. (Ed) Gondwana Eight, Assembly, Evolution and Dispersal, pp. 29–42. Balkema.

Cordani, U. G., Brito Neves, B. B., 1982. The geologic evolution of South America during the Archean and Early Proterozoic. Rev. Bras. Geoci. 12, 78–88.

Cordani, U. G., Iyer, S. S., Taylor, P. N., Kawashita, K., Sato, K., McReath, I., 1992. Pb–Pb, Rb–Sr, K–Ar systematics of the Lagoa Real uranium province (south central Bahia, Brazil) and the Espinhaço cycle (*ca* 1.5–1.0 Ga). J. South Amer. Earth Sci. 5, 33–46.

D'Agrella Filho, M. S., Pacca, I. G., Teixeira, W., Onstott, T. C., Renne, P. R., 1990. Paleomagnetic evidence for the evolution of Meso to Neo Proterozoic glaciogenic rocks in central–eastern Brazil. Paleogeog. Paleoclim. Paleoecol. 80, 255–265.

Dardenne, M. A., 1978. Sintese sobre a estratigrafia do Grupo Bambuí no Brasil Central. Bras. Geol. Congr., 30, Recife, Anais, SBG 2, 597–610.

Faure G., 1986. Principles of Isotope Geology, 2nd Edit. Wiley, New York.

Fuzikawa, K., Alves, J. V., Maruejol, M. L., Braz, E. R. C., Montes, A. de S. S., Oliveira, F. L. L., Ghignone, J. L., Silva, O., Jr, Castro, H. E. F., 1988. The Lagoa Real uranium province, Bahia State, Brazil, Some petrographic and fluid inclusion studies. Geochim. Bras. 2, 109–118.

Gascoyne, M., Stroes-Gascoyne, S., Sargent, F. P., 1995. Geochemical influence on the design, construction and operation of a nuclear waste vault. Appl. Geochem. 10, 657–671.

Han K. W., Heinonen J., Bonne A., 1997. Radioactive waste disposal: global experiences and challenges. IAEA Bull. 39/1.

Ivanovich M., Harmon, R. S. (Eds.), 1987. Uranium series disequilibrium: applications to environmental problems. Clarendon Press, Oxford.

Iyer, S. S., Babinski, M., Krouse, H. R., Chemale, F., 1995. Highly ^{13}C enriched carbonates and organic matter in the Neoproterozoic sediments of the Bambuí Group, Brazil. Precamb. Res. 73, 271–282.

Iyer S. S., Krouse H. R., Babinski M., 1992. Highly ^{13}C enriched carbonate and organic matter in the Neoproterozoic sediments of the Bambuí Group, Brazil. In 23 International Geological Congress, Kyoto, Japan, Proc. Vol. 1.

Kastenburg, W. E., Granton, L. J., 1997. Hazards of managing and disposing of nuclear waste. Physics Today 50, 41–47.

Kerrich, R., 1986a. Fluid transport in lineaments. Phil. Trans. R. Soc. Lond. A317, 219–251.

Kerrich, R., 1986b. Fluid infiltrations into fault zones: chemical, isotopic and mechanical effects. Appl. Geophys. 124, 225–268.

Levinthal J. S., Nagy B. and Gauthier-Lafaye F. 1989. Preliminary results from microanalysis of organic matter in the Lower Proterozoic uranium ores at Oklo in Gabon. U.S. Geol. Survey Open-File Report 89-668.

Lobato, L. M., Forman, J. M. A., Fuzikawa, K., Fyfe, W. S., Kerrich, R., 1982. Uranium enrichment in Archean crustal basement with overthrusting. Nature 503, 235–237.

Lobato, L. M., Fyfe, W. S., 1990. Metamorphism, metasomatism and mineralization at Lagoa Real, Bahia, Brazil. Econ. Geol. 85, 968–989.

Marinho M. M., 1991. La sequence volcano-sedimentaire Contendas–Mirante et la bordure occidantale du bloc Jequie (craton du São Francisco, Bresil): un examplo de transition Archean–Proterozoique, unpubl. Ph.D. thesis, Univ. Clermont-Ferrand, Paris, France.

Marinho, M. M., Vidal, Ph., Alibert, C., Barbosa, J. S. F., Sabaté, P., 1995. Geochronology of the Jequié–Itabuna belt and of the Contendas–Mirante volcano–sedimentary belt. Bol. Inst. Geoci. Universidade de São Paulo, Spec. Publ. 17, 75–96.

Maruejol, P., Cuney, M., Fuzikawa, K., Netto, A. M., Poty, B., 1987. The Lagoa Real Sub-alkaline complex, (South Bahia, Brazil): a source for uranium mineralization associated with Na–Ca metasomatism. Rev. Bras. Geoc. 17, 574–594.

Menager, M. T., Petit, J. C., Brocandel, M., 1992. The migration of radionuclides in granites: a review based on natural analogues. Appl. Geochem. 1 (Suppl), 217–238.

Nagy, B., Guthrie-Lafaye, F., Holliger, P., Mossman, D. J., Levinthal, J. S., Rigali, M. J., 1993. Role of organic carbon in the Proterozoic Oklo natural fission reactor, Gabon, Africa. Geology 21, 655–658.

Parenti Couto, J. G., Cordani, U. G., Kawashita, K., Iyer, S. S., Moraes, N. M. P., 1981. Consideraçoes sobre a idade do Grupo Bambuí com base em analises isotopicas de Sr e Pb. Rev. Bras. Geoc. 11, 5–16.

Pertlik F., Rogers J. J. W., Adams J. A. S., Haack U. K., 1978. Uranium. In Wedepohl, K. H. (Ed) Handbook of Geochemistry 92A1-920. Springer-Verlag.

Renne, P. R., Onstott, T. C., D'Argella Filho, M. S., Pacca, I. G., Teixeira, W., 1990. $^{40}Ar/^{39}Ar$ dating of 1.0–1.1 Ga magnetization from the São Francisco and Kalahari Cratons: tectonic implications for Pan-African and Brasiliano mobile belts. Earth Planet. Sci. Lett. 101, 349–366.

Rosholt, J. N., Zartman, R. E., Nkomo, L. T., 1973. Lead isotope systematics and uranium depletion in Granite Mountain, Wyoming. Geol. Soc. Amer. Bull. 84, 982–1002.

Stacey, J. C., Kramers, J. D., 1975. Approximation of lead isotope evolution by a two stage model. Earth Planet Sci. Lett. 26, 207–221.

Stein J. H., Neto A. M., Drumond A., Angeiras A. G., 1980. Nota preliminar sobre os processos de albitizacao uranifera de Lagoa Real (Bahia) e sua comparação com os de URSS e Suecia. In Bras. Geol. Congr., 32, Camboriu, Anais. SBG. **3**, 1758–1775.

Thomaz Filho, A., Bonhomme, M. G., 1979. Datations isotopiques Rb–Sr et K–Ar dans le Groupe Bambuí a São Francisco (MG) au Bresil. Phase metamorphique bresilienne synchronne de la primiere phase panafricain. C. R. Acad. Sci. Ser. D 299, 1221–1224.

Thomaz Filho, A., Lima, V. Q., 1981. Datação radiometricas de rochas peliticas pelo metodo Rb–Sr. Bol. Petrobras, Rio de Janeiro 24, 109–119.

Turpin, L., Maruejol, P., Cuney, M., 1988. U–Pb, Rb–Sr and Sm–Nd chronology of basement hydrothermal albitites and uranium mineralization, Lagoa Real, South Bahia, Brazil. Contrib. Mineral. Petrol 98, 139–147.

Villaça, J. N., 1982. Distrito uranifero de Lagoa Real—Reservas e potencial. Anais. Congr. Bras. Geociencias 32, Salvador, Bahia 5, 2048–2061.